MINISTÉRIO DA CIÊNCIA E TECNOLOGIA
INSTITUTO DE PESQUISAS ESPACIAIS

AUTORIZAÇÃO PARA PUBLICAÇÃO
AUTHORIZATION FOR PUBLICATION

PALAVRAS CHAVES/KEY WORDS
AUTORES/AUTHORS
SOLAR WIND-MAGNETOSPHERE
COUPLING
GEOMAGNETIC STORMS

AUTORIZADA POR/AUTHORIZED BY
V.W.J.H. Kirchhoff
Director Space Atmos. Sci.

AUTOR RESPONSAVEL
RESPONSIBLE AUTHOR
Walter D. Gonzalez

DISTRIBUIÇÃO/DISTRIBUTION
☐ INTERNA / INTERNAL
☒ EXTERNA / EXTERNAL
☐ RESTRITA / RESTRICTED

REVISADA POR/REVISED BY
Osmar Pinto Jr.
Editor Space Atmos. Sci.

CDU/UDC
523.3.4-854

DATA/DATE
August 1988

PUBLICAÇÃO Nº
PUBLICATION NO
INPE-4676-PRE/1373

ORIGEM
ORIGIN
DGE

PROJETO
PROJECT
MAGNET

Nº DE PAG.
NO OF PAGES
44

ULTIMA PAG.
LAST PAGE
43

VERSÃO
VERSION

Nº DE MAPAS
NO OF MAPS

TÍTULO/TITLE

SOLAR WIND-MAGNETOSPHERE COUPLING DURING INTENSE MAGNETIC STORMS (1978-1979)

AUTORES/AUTHORSHIP

W.D. Gonzalez
Bruce T. Tsurutani
Alicia L.C. Gonzalez
Edward J. Smith
Frances Tang
Syun-I, Akasofu

RESUMO-NOTAS/ABSTRACT-NOTES

The solar wind-magnetosphere coupling problem is investigated for the ten intense magnetic storms (Dst < -100 nT) that occurred during the 500 days (August 16, 1978 to December 28, 1979) studied by Gonzalez and Tsurutani (1987). This investigation concentrates on the ring current energization in terms of solar wind parameters, in order to explain the |-Dst| growth observed during these storms. Thus several coupling functions are tested as energy input and serveral setes of the ring current decay time-constant are searched to find best correlations with the Dst response. From the fairly large correlation coefficients found in this study, there is strong evidence that large scale magnetospause reconnection operates during such intense storm events and that the solar wind ram pressure plays an important role in the ring current energization. Thus a ram pressure correction factor is suggested for expressions concerning the reconnection power during time intervals with large ram pressure variations. The best set of values found from the present study is in accord with recent similar and independent suggestions. With respect to the ring current energy injection rates during intense storm events, typical values of 150 ± 50 nT/hour are obtained. These are considerably larger than values extrapolated from previous studies restricted to moderate storms. Such rates of energy injection are observed to get transmitted from the magnetopause to the inner magnetosphere with an average time delay of about 1 hour, although this delay can become shorter as the storm events get more intense.

OBSERVAÇÕES/REMARKS

This work was published in J. Geophys. Res., Vol. 94, nº A7, 8835, 1989.

MINISTÉRIO DA CIÊNCIA E TECNOLOGIA
INSTITUTO DE PESQUISAS ESPACIAIS

PROPOSTA PARA PUBLICAÇÃO

- [ ] DISSERTAÇÃO
- [ ] TESE
- [x] RELATÓRIO
- [ ] OUTROS

IDENTIFICAÇÃO

TÍTULO

"SOLAR WIND-MAGNETOSPHERE COUPLING DURING INTENSE MAGNETIC STORMS (1978-1979)"

AUTOR(ES)

Walter D. Gonzalez
Bruce T. Tsurutani
Alicia L.C. Gonzalez
Edward J. Smith
Frances Tange
Syun I. Akasofu

ORIENTADOR (DISS. OU TESE)

CO-ORIENTADOR

LIMITE	DEFESA	CURSO	ÓRGÃO
__/__/__	__/__/__		

DIVULGAÇÃO

- [x] EXTERNA
- [ ] INTERNA
- [ ] RESTRITA

EVENTO/MEIO

- [ ] CONGRESSO
- [ ] REVISTA
- [ ] OUTROS

REV. TÉCNICA

NOME DO REVISOR: Osmar Pinto Junior

RECEBIDO	DEVOLVIDO	ASSINATURA
3/8/88	8/8/88	Osmar Pinto J.

APROVAÇÃO

NOME DO RESPONSÁVEL: José Marques da Costa

APROVADO	DATA	ASSINATURA
[x] SIM [ ] NÃO	04/8/88	J. M. - DCA

REV. LINGUAGEM

Nº PRIOR.	RECEBIDO	NOME DO REVISOR
	__/__/__	

PÁG.	DEVOLVIDO	ASSINATURA
	__/__/__	

DATILOGRAFIA

OS AUTORES DEVEM MENCIONAR NO VERSO INSTRUÇÕES ESPECÍFICAS, ANEXANDO NORMAS, SE HOUVER

RECEBIDO	DEVOLVIDO	NOME DA DATILÓGRAFA
	__/__/__	

DIRETOR

AUTORIZO A PUBLICAÇÃO

- [ ] SIM
- [ ] NÃO

08/8/88

Nº DA PUBLICAÇÃO: 4676 PRE/1879 PÁG.:
CÓPIAS: Nº DISCO: LOCAL:

OBSERVAÇÕES E NOTAS

O trabalho será submetido para a JGR

Autorizo a dispensa de Revisão de Linguagem

JOSÉ MARQUES DA COSTA
Chefe do Departamento de Geofísica e Aeronomia-DGA

APÓS A PUBLICAÇÃO, ESTA FICHA SERÁ ARQUIVADA JUNTAMENTE COM A VERSÃO ORIGINAL

INPE 106

SOLAR WIND-MAGNETOSPHERE COUPLING DURING INTENSE MAGNETIC STORMS (1978-1979)

Walter D. Gonzalez[1], Bruce T. Tsurutani[2], Alicia L.C. Gonzalez[1], Edward J. Smith[2], Frances Tang[3], and Syun-I. Akasofu[4]

ABSTRACT The solar wind-magnetosphere coupling problem is investigated for the ten intense magnetic storms (Dst <-100 nT) that occurred during the 500 days (August 16, 1978 to December 28, 1979) studied by Gonzalez and Tsurutani [1987]. This investigation concentrates on the ring current energization in terms of solar wind parameters, in order to explain the |-Dst| growth observed during these storms. Thus several coupling functions are tested as energy input and several sets of the ring current decay time-constant τ are searched to find best correlations with the Dst response. From the fairly large correlation coefficients found in this study, there is strong evidence that large scale magnetopause reconnection operates during such intense storm events and that the solar wind ram pressure plays an important role in the ring current energization. Thus a ram pressure correction factor is suggested for expressions concerning the reconnection power during time intervals with large ram pressure variations. The best set of values found from the present study is in accord with recent similar and independent suggestions. With respect to the ring current energy injection rates during intense storm events, typical values of 150 ± 50 nT/hour are obtained. These are considerably larger than values extrapolated from previous studies restricted to moderate storms. Such rates of energy injection are observed to get transmitted from the magnetopause to the inner magnetosphere with an average time delay of about 1 hour, although this delay can become shorter as the storm events get more intense. It is also found that AE does not respond as well as Dst to the coupling functions, except for the events that have Dst values only >-100 nT (less intense energization). This point suggests that there is a decoupling between the ring current and auroral processes during very intense storms with respect to their dependence on solar wind energization. Finally, a discussion is presented on associations of the coupling functions with the solar wind features described by Tsurutani

et al. [1988] for the causes of these storm events.

1. Introduction

The works by Tsurutani et al. [1988] and by Tang et al. [1989] deal with interplanetary and solar causes of the 10 intense geomagnetic storms (Dst < -100 nT) that occurred in the interval August 16, 1978, to December 28, 1979. These events were documented and discussed by Gonzalez and Tsurutani [1987] with the use of Dst data together with interplanetary magnetic field and plasma data collected by the ISEE 3 satellite, while it was in front of the Earth in its halo orbit about the L_1 libration point. Gonzalez and Tsurutani [1987] have claimed that a common interplanetary feature for these storm events were long-duration (>3 hours), large and negative (<-10 nT) interplanetary magnetic field (IMF) B_z events, associated with interplanetary duskward electric fields > 5 mV/m.

It is the purpose of the present paper to study the "solar wind-magnetospheric coupling" problem during those storm-events, with specific focus on ring current energization dependence on solar wind parameters. Previous studies of this type have mainly concentrated on a single coupling function [Perreault and Akasofu, 1978] and/or on storms of moderate intensity [Burton et al., 1975; Murayama, 1982; Feldstein et al., 1984; Pudovkin et al., 1985]. Thus we expect that the present study will extend previous results to intense storms, with particular attention to the role of several candidate coupling functions for ring current energization. Furthermore, since it has been claimed that the ring current decay time-constant, not well known as yet, plays an important role in the ring current energy dissipation [e.g., Vasyliunas, 1987], the present study will also try to focus on this important parameter.

In section 2, a summary of the ten intense storm events is presented, along with a discussion on some aspects relevant to their geomagnetic activity behavior.

After reviewing the dynamics of ring current energization as well as several suggested solar wind-magnetosphere coupling functions [e.g., Burton et al., 1975; Perreault and Akasofu, 1978; Vasyliunas et al., 1982; Bargatze et al., 1986; Murayama, 1986; Gonzalez, 1986], we study in section 3 the evolution of the ring current during the main phase of the intense storm events. Each of the selected coupling functions is assumed to be directly associated with energy

input during such evolution. Particular importance is given to the role of the solar wind ram pressure in magnetospheric energization, expected to exist according to past solar wind-magnetosphere studies [e.g., Murayama, 1982; Gonzalez and Gonzalez, 1984] and experimental evidence [e.g., Tsurutani et al., 1985; Smith et al., 1986; Gonzalez et al., 1989]. In this section, a study of AE response to the same coupling functions and for the same time intervals selected for the ring current response investigation is presented.

Section 4 provides a discussion on several aspects suggested by the results obtained in section 3. Section 5 gives a summary of the main conclusions.

For the present study we have used 5-min averages, both for the Dst data as well as for the ISEE 3 measured solar wind parameters. We have also assumed that during the events of the present study, the large-scale and long-duration interplanetary events convected from the ISEE 3 location to the magnetopause without any appreciable change, as concluded by Kelly et al. [1986].

2. Intense Storm Events (1978-1979)

An overview of the 10 intense storm events, with Dst $\leq$-100 nT, that occurred in the interval August 16, 1978, to December 28, 1979, is given on Figure 1 (taken from Gonzalez and Tsurutani [1987]). From left to right are: the interplanetary phenomena detected prior to the large southward IMF event causing the magnetic storms (Mach number, if shocks), peak southward B_z and IMF magnitudes and peak Dst values. All southward events occurred within 36 hours of a leading interplanetary shock (nine out of ten events) or a noncompressive density enhancement event (one case). For more details about the interplanetary cause of these storm events the reader is referred to Tsurutani et al. [1988].

Figure 2 refers to the storm event of September 29, 1978, and illustrates the interplanetary plasma and magnetic field data, detected by ISEE 3, as well as the geomagnetic activity data (AE and Dst) used in our study. From top to bottom are the helium density, proton temperature, velocity and density, the IMF Y and Z components (in solar magnetospheric coordinates) and IMF magnitude, and the magnetospheric parameters AE and Dst. For more details about the ISEE 3 measurements and method of analysis of the interplanetary data, the reader is referred to Frandsen et al. [1978],

Bame et al. [1978], and Tsurutani et al. [1988]. The AE and Dst plots were obtained in a manner similar to that described by Baker et al. [1983].

Event Case Study

For brevity, a description about the behavior of Dst and of some interplanetary parameters is given below only for some selected events, for which a full set of interplanetary and magnetospheric data is shown on Figures 2, 3, and 4. They are the events on September 29, 1978, November 25, 1978, and September 18, 1979, and represent the different type of events encountered in our study with respect to interplanetary drivers and Dst complexity. The description will concentrate on the Dst growth in response to interplanetary conditions.

Table 1 gives a summary of some representative parameters for the 10 storm events. They are the selected time interval for the study of the Dst growth (the criteria for this selection is explained in section 3), the peak Dst value, and the average values of B_z, of the solar wind speed V and of the solar wind ram pressure p. As it will be shown in the following sections, these three interplanetary parameters play the major role in the ring current energization during the studied events. Note that days February 21, 1979, and March 29, 1979, include a secondary event (marked with a cross) that preceded the main event (not originally included in the 10 events) and, in both cases, the corresponding peak Dst reached values near -100 nT. Due to data gaps during the events of April 25, 1979, and of September 18, 1979 (marked with an asterisk), the selected intervals represent only partially the time interval of Dst growth.

September 29, 1978. This event is illustrated on Figure 2. The Dst growth follows the recovery phase of a previous storm, that occurred on day 25, and reaches a peak value of -215 nT at about 1100 UT on day 29. After the interplanetary shock was observed at about 2100 UT of day 28, the interplanetary parameters V and $-B_z$ reached fairly large amplitudes during the growth of the storm. B_z had values <-10 nT for more than 7 consecutive hours and a fairly broad peak at -24 nT between about 0830 UT and 1130 UT. It is interesting to note that the Dst parameter also showed a broad peak during this event. Although there is a data gap in the solar wind parameters, between approximately 0200 UT and

0500 UT, the large negative B_z turning at about 0600 UT is correlated with the rapid growth of the storm. Thus according to the criterion assumed in the following section for the selection of (main phase) storm intervals to study the Dst growth, the selected interval for this event was from 0700 UT to 1100 UT. Note that Dst started to grow already from a fairly moderate value at about -60 nT, due to the active interval that preceded the storm. Also note that the storm started its recovery phase at the same time as the B_z values became >-10 nT.

November 25, 1978. This event is illustrated on Figure 3. The interplanetary shock that occurred at about noon of November 25 seems to have amplified previously existing, already large, negative B_z fields [Tsurutani et al., 1988] and also seems to have started the main storm event of this day. Thus the -Dst values that exist previous to the main storm event are also correspondingly fairly large, with a peak value around -80 nT and a (moderate) Dst value of about -50 nT during the onset of the main storm event. Therefore this is an example of a complex (double) Dst event or even of a multiple one, if one also considers the Dst behavior on the previous day (November 24). The B_z field during the main event has values <-10 nT for about 5 consecutive hours, with a peak value of -16 nT. The peak Dst value during this main event was -150 nT. After a net lag of about 1 hour, the rapid turning of B_z to less negative values is correlated with the recovery of the storm. This time lag is in addition to that corresponding to the solar wind transit time from the ISEE 3 satelite to the Earth's magnetopause, which typically is also around 1 hour (see further related comments on section 3). The selected interval for the study of Dst growth during this event is from 1300 UT to 1900 UT.

September 18, 1979. This event is illustrated on Figure 4. It is different than the events described above, in that this event does not involve an interplanetary shock, but seems to follow a noncompressive density enhancement event [Gosling et al., 1977; Tsurutani et al., 1988]. Due to a fairly large data gap in the ISEE 3 data, we have selected the interval 0000 UT to 0800 UT for the study of the Dst growth. Therefore such growth is studied only partially, including the storm onset and a Dst growth until about -100 nT. The storm follows a quiet Dst period that existed for several

previous days. The B_z field had two large negative incursions. The first one with values <-10 nT during about 2 hours leading to Dst values around -60 nT. The second one with a longer negative incursion and apparently larger amplitudes (data gap), leading to a storm with a peak Dst value of -150 nT. Although the solar wind speed is relatively low, as compared to the values reached during the other events, the solar wind density was much higher than average (by a factor of 3 or more), associated with the non compressive density enhancement event that occurred during this interval. About an hour after B_z changed (rapidly) to positive values, the storm seems to have started its recovery phase.

In order to have an idea of the other events, the reader is referred to Figure 1 and to Table 1, which provide information on some important parameters for all 10 events as well as for the secondary events of days February 21, 1979, and March 29, 1979.

3. Ring Current Energization

For ring current energization studies the expression for the corresponding energy balance [following Burton et al., 1975; Akasofu, 1981] is usually written as

$$dU/dt = U_o - U/\tau \qquad (1a)$$

where U is the total kinetic energy of the particles, U_o the energy imput and τ the exponential time constant for energy decay. U can be related to the local time averaged perturbation field at the surface of the Earth, D, through the Dessler-Parker-Sckopke relation [Sckopke, 1966] as

$$D = -2/3\ (U/U_B)\ B_S$$

where U_B is the energy of the dipole magnetic field above the Earth's surface and B_S is the equatorial dipole field strength at the Earth's surface.

Thus using this relation in (1a) one gets

$$dD/dt = Q - D/\tau \qquad (1b)$$

with $Q = 2.5 \times 10^{-21}\ U_o$ (in Gaussian units), and D in nT. Thus

$$U_o = 4 \times 10^{20}\ (d/dt + 1/\tau)\ D \qquad (1c)$$

Usually, D is related to the storm parameter Dst through:

$$D = Dst - b\,(p)^{1/2} + c \qquad (2)$$

[e.g., Burton et al., 1975; Akasofu, 1981; Feldstein et al., 1984], where p is the (disturbed day) ram pressure of the solar wind, namely ρV^2, with ρ and V being the solar wind mass density and speed, respectively, b is a proportionality constant, and c represents the quiet-day contribution to D. From studies by Burton et al. [1975], Feldstein et al. [1984] and others, the approximate values of b and c are

$$b = 0.2\ nT/(eV\ cm^{-3})^{1/2}$$

$$c = 20\ nT$$

Therefore from measurements of the Dst index and of the solar wind ram pressure, and assuming that the energy input function Q depends basically on solar wind parameters, one can try to find the combination of solar wind parameters (coupling function) that better explains the evolution of Dst. However, since τ is not well known as yet [e.g., Akasofu, 1981, 1986; Zwickl et al., 1987; Vasyliunas, 1987], some assumption about the values of this parameter needs to be made. This will be described later in this section.

Following the above scheme several authors, e.g., Burton et al. [1975], Perreault and Akasofu [1978], Feldstein et al. [1984], Pudovkin et al. [1985], Murayama [1982, 1986], and Fay et al. [1986] have studied the storm response to interplanetary-magnetosphere coupling functions, although restricted to moderate storms and/or to isolated coupling functions. The Dst < -100 nT threshold, used by Gonzalez and Tsurutani [1987] and in the present work to characterize intense storms, has been already used before by other authors [e.g., Akasofu, 1981]. It also has been adopted by the Solar Geophysical Data Journal as a practical measure for a similar definition.

Burton et al. [1975] restricted their Dst-solar wind coupling study to the "rectified" electric field function VB_z, assumed to give finite energization only for negative values of B_z. This restriction was relaxed by Feldstein et al. [1984] showing that finite energization also exists for a range of positive values of B_z. For their coupling study, Perreault and Akasofu [1978] defined an empirical coupling function related to the magnetopause reconnection power

[e.g., Kan and Lee, 1979; Gonzalez, 1986]. Such function was called $\epsilon = L_0^2 V B^2 \sin^4(\theta/2)$, where B is the IMF amplitude, L_0 is a constant (approximately equal to 7 Earth radii) and θ is the "clock angle" between the z axis and the transverse component of the IMF vector, $\underline{B}_T = \underline{B}_z + \underline{B}_y$, in solar magnetopheric coordinates [e.g., Gonzalez and Mozer, 1974]. Pudovkin et al. [1985] tried several other coupling functions, although their study was restricted to the peak Dst values of the storms. They found better correlations for VB_z and for the dawn-dusk component of the reconnection electric field, $VB_T \sin^2(\theta/2)$, at the limit of equal reconnecting field amplitudes [Gonzalez, 1986]. Murayama [1982, 1986] and Maezawa and Murayama [1986] tested the coupling functions VB_z, V^2B_z and $V^a B_z^b \rho^c$, where ρ is the solar wind mass density and a, b and c are coupling exponents. Their best correlations were found for a function approximately given by $V^2 B \rho^{0.4}$. This function incorporates the solar wind ram pressure as an important parameter in the coupling. Fay et al. [1986] tested the VB_z and ρV^2 functions separately using the technique of linear prediction filters [Iyemori et al., 1979; Clauer, 1986], showing that these functions together can account for about 70% of the Dst variance.

Thus in summary, the following functions have been previously tested for ring current energization:

$$V B_z \tag{3a}$$

$$V B_T \sin^2(\theta/2) \tag{3b}$$

$$\epsilon = L_0^2 V B^2 \sin^4(\theta/2) \tag{4}$$

$$\rho^{1/2} V B_z \ (\sim \rho^{0.4} V^2 B_z) \tag{5}$$

All these functions, except perhaps (1a), have also been used in correlation studies with auroral indices [e.g., Akasofu, 1981; Baker et al., 1983; Tsurutani et al., 1985; Maezawa and Murayama, 1986]. However, Bargatze et al. [1986] found that a function that correlated best with the auroral index AL has the form

$$\rho^{1/6} V B \sin^4(\theta/2) \tag{6}$$

Apparently this latter function has not been tested, as yet, for correlation studies with Dst.

Gonzalez [1986] has shown that the above expressions (3a), (3b) and (4) are limits of the

following more general expressions on electric field and energy transfer due to magnetopause reconnection.

$$E_D(s,\theta) = (1/c)\ V\ B_T\ (s-\cos\theta)^{-1}\ K(s,\theta) \quad (7)$$

$$P_D(s,\theta) = (1/\pi)\ V\ L^2\ B_T\ B_M\ K(s,\theta) \quad (8)$$

with

$$K(s,\theta)=(1-s\ \cos\theta)(s-\cos\theta)^2/(1+s^2-2s\ \cos\theta) \quad (9)$$

where E_D and P_D are (in Gaussian units) the electric field and power related to the dawn-dusk component of the reconnection electric field [Gonzalez and Mozer, 1974; Gonzalez and Gonzalez, 1981]. L is the magnetopause radius at the nose, $s = |\underline{B}_G|/|\underline{B}_M| \geq 1$, with $\underline{B}_G$ and $\underline{B}_M$, being respectively, the geomagnetic and magnetosheath magnetic fields at the magnetopause. In these expressions $1 \geq s\ \cos\theta$, otherwise $E_D=P_D=0$. Function (6) can also be shown [Gonzalez, 1988] to be another limit of the general expression (8). A meaning of function (5) is discussed in the following section.

From dimensional analysis, Vasyliunas et al. [1982] have shown that, in order to represent power, expressions of the $VB_zG(\theta)$ type are dimensionally correct when multiplied by the factor $p^{1/6}$. Similarly, expressions of the ϵ type are dimensionally correct when multiplied by the factor $p^{-1/3}$. Note that from the above given functions, only expression (6) satisfies such a requirement. If $a = 1/4$ and $G(\theta) = 1$ in equation (12) of Vasyliunas et al. [1982], one gets the following dimensionally correct and alternative expression for the coupling power:

$$p^{1/2}\ V\ B_T^{1/2} \quad (10)$$

Thus the coupling function (5), $p^{1/2}VB_z$, is dimensionally incorrect, although it has been successfully used in the literature [Murayama, 1986].

Note, however, that it is possible to place a constant in each power expression with the proper units in order to satisfy the dimensionality argued by Vasyliunas et al. [1982]. Therefore the corrections mentioned above are intended more to satisfy the scaling relations discussed by Vasyliunas et al. [1982], that resulted from assuming a power law dependence of the coupling power on B_T, thus fixing its dependence on the other solar wind parameters, except θ.

In our present work we have tested: functions (3) and (4) and their corresponding expressions when corrected dimensionally; functions (5), (6) and (10); and several others similar functions listed in the appendix including function (3b) dimensionally corrected. Some of these functions have been suggested by Gonzalez [1986] and the others are variations of (5) and (6) involving different angular factors. As listed in the appendix, functions involving $B_z \sin^n(\theta/2)$, $B_z^2 \sin^n(\theta/2)$ and B_T without an angular factor have been examined as additional combinations, although they are not expected from standard reconnection models. However, they could gain perhaps more sense in alternative models of solar wind-magnetosphere interaction, involving or not magnetospheric reconnection. The function $p^{1/6} V B_T \sin^4(\theta/2)$ has been examined in addition to $p^{1/6} V B \sin^4(\theta/2)$ because B_T could modulate the coupling function differently than B for the same angle θ. Besides, VB_T is a better definition than VB for the interplanetery electric field.

We have also tested the general expression (8) for reconnection power as a coupling function with the following approximations:

$L = L_{CF}$, the Chapman-Ferraro scale length, with $L_{CF} \propto p^{-1/3}$;

$B_M = 2(B_T B_G)^{1/2}$, the Crooker et al. [1982] compression parameter;

$B_G = (8\pi\rho V^2 + B^2)^{1/2}$, from pressure balance at the magnetopause.

Thus equation (8) gives

$$P \propto p^{-1/3} V B_T B_M K(s,\theta) \qquad (8')$$

Note that the dimensionally correct version of ε can be derived from (8') when s tends to 1 [Gonzalez, 1988], in a similar manner done [Gonzalez and Gonzalez, 1984] for (4) from (8).

In the following section, we have called E the electric field function (3) and have grouped the functions of the electric field type, like equation (6), under the general symbol E'. Expression (5) has been called P to designate its strong dependence ($p^{1/2}$) on the solar wind ram pressure and all other functions with the same dependence have been referred as P'. Finally, the general expression (8') for the reconnection power has been called R. This nomenclature is also shown in Table 2.

Best Coupling Functions for Intense Storms

The above given coupling functions, generally called F, have been assumed to represent the power input Q in equation (1a), such that $Q = AF + B$, with A and B being fitting parameters. Thus $(dD/dt + D/\tau)$ values were compared to Q values from measurements of Dst and solar wind parameters in order to look, from a linear fit analysis, for the best coupling functions using the assumptions listed below. However, in order to perform this analysis, best values of the time constant τ were also sought instead of assumed. Burton et al. [1975], Perreault and Akasofu [1978] and Murayama [1982] used constant values for τ of the order of 8 to 12 hours for all phases of their studied storms. Pudovkin et al. [1985] used a constant value of $\tau = 4$ hours for the growth phase of their studied storms. Similar values were used by Feldstein et al. [1984], although they adopted a set of two values for different regimes of Dst, namely, $\tau = 8$ hours for $Dst \geq -55$ nT and $\tau = 6$ hours for $-120 \leq Dst < -55$ nT. On the other hand, Akasofu [1981] and Vasyliunas [1987] have suggested a much larger domain for the τ variability, depending on the regime of ring current energy input, Q. This domain involves values of τ as small as 0.25 hours and as large as 20 hours. From equation (1b), with $D/\tau \gg dD/dt$ for intense storms [e.g., Zwickl et al., 1987], the works of Akasofu [1981] and Vasyliunas [1987] also suggest that the values of τ tend to decrease with increasing values of $|-Dst|$.

Thus combining those previous studies on τ, we have assumed three domains of Dst in order to search for the corresponding best values of τ from the correlation study. They are

$$Dst \geq -50 \text{ nT}$$

$$-120 \leq Dst < -50 \text{ nT}$$

$$Dst < -120 \text{ nT}$$

We started with the following sets of equal τ values (in hours) for the three domains: (8,8,8), (6,6,6), and (4,4,4), for each of the tested coupling functions. Since the resulting correlation coefficients were low (usually <0.5), we tested sets of τ values that decrease when $|-Dst|$ increases, such as (8,4,1), (6,2,0.5), (4,0.5,0.25) and a few more. We noticed inmediately that all coupling functions showed much better correlation coefficients for the sets (4,0.5,0.5) and (4,0.5,0.25). Because we have been working with about 24 coupling

functions and the correlation coefficients were already quite large, we stayed with these latter sets of τ values. Therefore refinements around these values have not been tried as yet. A justification about the vality of these τ values is given in the following section by comparing them with similar recent and independent results.

The following assumptions have been used in the linear fit analysis of equation (16):

The study of the Dst evolution was restricted only to the storm time interval that corresponds to the growth of the ring current intensity (main phase), since it is during this interval of time that the energy input and, therefore, the coupling function can be better studied [Burton et al., 1975; Feldstein et al., 1984; Pudovkin et al., 1985]. This restriction was also based on the interest of studying only intense injection events. Additional but minor injection events were observed to be sometimes present during the recovery phase of the intense events, thus providing a different regime of energy injection. Those minor injection events were always associated to the presence of $|-B_z|$ fields of only a few nT.

The initial time (storm onset) for studying the Dst growth, during each event, was selected at the time of the lowest value of $|-Dst|$, usually around prestorm values, from which Dst was notably decreasing (main phase) till the occurrence of the peak Dst value of the storm. Main phase duration intervals for the studied events varied from a few hours up to about half a day. When gaps existed in the solar wind data, this selection criterion was followed only partially, but as close as possible.

A constant delay time of one hour was adopted between the observed time of solar wind parameters at the ISEE 3 location and their expected arrival time at the magnetopause [Gonzalez and Tsurutani, 1987]. Furthermore, the long-duration and large-scale interplanetary features involved in the present study were assumed to convect to the magnetopause practically without change from the ISEE 3 location [Kelly et al., 1986].

All possible time lags between the coupling function at the magnetopause and the ring current evolution have been incorporated in a variable lag of the function F with respect to D. This variable lag was studied in steps of 5 min. However, the propagation of pressure changes from the magnetopause to the inner magnetosphere, directly influencing D (equation 2), was assumed to occur with a zero time lag. This is justified by the much smaller time

delays observed [e.g., Fay et al., 1988] for the propagation of pressure changes (independent of convection), as compared to those usually observed for convection related parameters.

The data consisted of 5 min averages of the solar wind (ISEE 3) measurements and of the Dst and AE values. Because rapid fluctuations were present in the amplitude and components of the IMF, they have been smoothed with a running average at intervals of 30 min. This is justified by the commonly accepted fact that the magnetosphere probably does not respond to rapid changes (within <30 min) of the IMF [e.g., Burton et al., 1975; Vasyliunas et al., 1982].

Therefore for each of the events, the coupling functions listed in Table 2 were tested in order to find best correlation coefficients for a linear fit of Q to ($dD/dt + D/\tau$) in equations (1b) and (2).

Table 3 is a summary of the best coupling functions for each of the studied events, in which the correlation coefficients, time lags (from magnetopause to the ring current) and best set of τ values are also given. The selected time interval for the storm growth, indicated in Table 1, is also shown for each event. The selected coupling functions are those that had the best correlation coefficients within a relative difference of at most 10% and up to a number of 5. Thus because this restriction, the number of selected best functions differ from event to event.

AE Response

Because the main objetive of this work is the study of the "ring current-interplanetary" coupling during intense storm events, and also because there is not, as yet, expressions similar to (1b) and (2) to study the AE time evolution as a function of solar wind parameters, we have only compared the response of AE values to the same coupling functions used in the Dst study. Table 4 shows the best coupling functions and time lags for each of the 10 events computed for the same time intervals used in the Dst study.

With respect to the relative importance of AE energy dissipation as compared to that for the ring current during intense storm events, it is also commonly believed that the AE contribution is practically negligible [e.g., Akasofu, 1981; Baker et al., 1983; Zwickl et al., 1987; Vasyliunas, 1987].

4. Discussion and Conclusions

Best Coupling Functions

From the results shown in Table 3, one observes that there are several coupling functions that give, for each event, similar correlation coefficients, which are among the best within a relative difference of 10%. However, some of those functions show up more frequently than the others, suggesting a better (more frequent) representation of the coupling. Thus the four more frequent functions are given in Table 5 together with the number of events in which they are present, their average time lags, their most common set of τ values and their average coupling constant <A>. Note that the selected function $E' = p^{1/6} VB \sin^4(\theta/2)$ is the most frequent one among the E' type functions, although other similar expressions are also fairly (but less) frequent in Table 3.

Table 6 gives the correlation coefficients for the four more frequent functions shown on Table 5 for each of the studied events. The numbers in boldface are those that also appear on Table 3 and have been used for the information shown in the second column of Table 5. From the numbers shown in Table 6 one observes that all the four functions have a similar validity for predicting the energization of intense storms. They all have similar correlation values, increasing or decreasing together from event to event. The possible reasons for their variability from event to event are discussed below, after some further considerations on these selected coupling functions are given.

The coupling constant B, in the linear fit $Q = AF + B$, was observed to have a large dispersion for individual cases. However, the average value <B> is negligible, compared with <A>F, for each of the selected functions of Table 5. This might suggest that $Q = 0$ when $F = 0$. However, this conclusion can not be drawn from our study, which was restricted only to intense storm events that mostly include large values of F. Thus to study the regime of low values of F, in order to find <B>, it would be necessary to include moderate storms as well.

What are the meaning of the four most common coupling functions of Table 5? What do they have in common? In which conditions does each of them tend to become better than the others? How are they associated to interplanetary features?. We try to provide below some answers for the first couple of questions, although we believe that it is somewhat premature to find clear answers to

the latter two, only from the 10 events presently studied.

The coupling functions of Table 5 are those given in section 3 by expressions (4), (5), (6) and (8'). These expressions correspond, respectively, to the function ϵ described by Perreault and Akasofu [1978] and Akasofu [1981], to the function $p^{1/2}VB_z$, which is similar to that given by Murayama [1986] and Maezawa and Murayama [1986], to the function $p^{1/6}VBsin^4(\theta/2)$ given by Bargatze et al. [1986] and to the general expression for the reconnection power $P_D(s,\theta)$ given by Gonzalez [1986]. The functions $P_D(s,\theta)$, $p^{1/6}VBsin^4(\theta/2)$ and $p^{1/2}VB_z$ have explicit dependences on the solar wind ram pressure p. The function $p^{1/2}VB_z$ can be thought as being the dimensionally correct electric field function $p^{1/6}VB_z$ [Vasyliunas et al., 1982] times the factor $p^{1/3}$, which is inversely proportional to the reconnection area in terms of the Chapman-Ferraro scale length, L_{CF}^2. This further pressure correction factor seems to be necessary because as pressure increases, the reconnection area diminishes.

Because $p^{1/6}VB_z$ is a special case of $p^{1/6}VB\ sin^4(\theta/2)$, whereas this latter function and ϵ are limits of $P_D(s,\theta)$ [Gonzalez, 1988], all these functions refer to the power transmitted to the magnetopause by the reconnection electric field at the magnetopause. Therefore one expects that under normal pressure conditions all four functions should give similar correlation coefficients, whereas during large pressure variations the ones that have stronger pressure dependence factors would represent better coupling.

An inspection of the Tables 1 and 3 with respect to pressure dependences seems to confirm this expectation, with functions modulated by the $p^{1/2}$ factor becoming dominant during events with large pressure variations (e.g., August 28, 1978; March 29, 1979; April 25, 1979). A further confirmation of this expectation has been also presented recently [Gonzalez et al., 1988].

This pressure dependence is shown in a more quantitative way in Figure 5, which gives the exponent of the ram pressure factor p of the best coupling functions, listed in Table 3, as a function of the relative ram pressure variability, given at the last column of Table 1 for each event. In this figure the crosses refer to the events with a clear evidence of the representative exponent of p in the selected functions, whereas the dots refer to the events when the selected functions showed practically a pressure independent behavior. Thus these latter

cases were plotted as if they had a zero-pressure exponent too. This figure suggests that the exponent of the ram pressure factor in the coupling functions tends to increase with the ram pressure variability.

The four best coupling functions of Table 5 encompass most of the successful coupling functions studied before with respect to ring current energization. One is of the electric field type [Burton et al., 1975; Feldstein et al., 1984; Pudovkin et al., 1985], one of the "pressure" type [Murayama, 1986; Maezawa and Murayama, 1986], one is ϵ [Perreault and Akasofu, 1978; Akasofu, 1981] and one is the general reconnection power function $P_D(s,\theta)$ studied by Gonzalez and Gonzalez [1984]. From Table 5 one can not say which of the four functions is the best, although the following two general conclusions can be advanced. One of them refers to the function $P_D(s,\theta)$. Because three of the best coupling functions can be derived from $P_D(s,\theta)$, except for the extra pressure correction factor in $p^{1/2}VB_z$, one could suggest that the function $P_D(s,\theta)$ is a candidate for a general coupling function to represent ring current energization. Aside from its complexity, one expects that this general function will represent the coupling even better when the approximations used in its computation improve with better knowledge of its composite parameters, especially the magnetosheath field B_M. In fact, judging from the propagation of errors of the parameters involved in the coupling functions, one would expect better results (correlation coefficients) for simpler functions, like VB_z, than for the more complex functions $P_D(s,\theta)$, contrary to what has been obtained. The other general conclusion refers to the role of the solar wind ram pressure in ring current energization. As suggested by the best representation of the coupling functions of the $p^{1/2}VB_z$ type during events with large pressure variations, it is advanced that a ram pressure modulation becomes important during such cases. Thus magnetopause reconnection models should incorporate such a modulation, because none of the (dimensionally correct) versions of the reconnection power have a strong dependence on ram pressure such as $p^{1/2}$.

From Table 5 one can also conclude that the average time lag for power transmission between the magnetopause and the inner magnetosphere is about 1 hour. However, Table 3 also indicates that this time lag tends to become shorter (longer) for more (less) intense storms.

From Table 3 one also observes that all coupling functions gave smaller correlation coefficients (around 0.6 to 0.8) for the events that involved large data gaps (April 25, 1979; August 29, 1979; September 18, 1979) or the lowest peak Dst values, close to -100 nT (February 21, 1979; March 29, 1979). Due to the data gaps, the selected time intervals for the former events also involved Dst values only >-100 nT. On the other hand, the AE values showed the best correlations exactly during these same cases, as shown in Table 4. Thus one possible explanation for the lower correlation events in Table 3 could be that, during less intense events, the magnetospheric energy input, represented by the function Q in equation (1b), needs a correction term proportional to AE [Akasofu, 1981; Zwickl et al., 1987; Vasyliunas, 1987]. Such correction term was neglected in our study, as commented in section 3, mainly because a functional form for AE, at the level of that for Dst, does not exist as yet.

An additional explanation for the lower correlation events could be that the ring current energization gets more and more controlled (driven) only by solar wind parameters the more intense the event becomes. Thus during less intense events, coupling functions involving only solar wind parameters would not be sufficient to explain the ring current energization and a combination of "driven" as well as of magnetospheric "unloading" processes [e.g., Rostoker et al., 1987] should be considered.

With respect to the AE reponse one can also note in Table 4 that the time lags for the best coupling functions are considerably smaller (with an average value of about 25 min) than those found for the ring current response. This is in agreement with several works on the response of auroral parameters to solar wind conditions [e.g., Baker, 1986].

The fact that AE correlates with the coupling functions much better during less intense storms than during more intense ones is in agreement with a similar result found by Baker et al. [1983]. This could imply a decoupling between the ring current and auroral processes during intense storms with respect to solar wind energization, as also suggested by the Akasofu [1981] work about a clear Dst-AE decoupling for intense storms. However, it is also possible that the AE index is not a good indicator for the Joule losses in the high-latitude ionosphere during intense storms, because maximum disturbances are observed at stations located at lati-

tudes lower than those of the AE stations (S. Kokobun, personal comunication, 1988).

Best Set of τ Values

From Table 3 the best set of τ values found in our correlation study was

$$\begin{aligned} \tau &= 4 \text{ hours, for} && Dst \geq -50 \text{ nT} \\ &= 0.5 \text{ hours, for} && -50 > Dst \geq -120 \text{ nT} \\ &= 0.25 \text{ hours, for} && Dst < -120 \text{ nT} \end{aligned}$$

Note that we have assumed a division of Dst and therefore also of τ only in three domains, for simplicity. However, since the obtained correlation coefficients were already sufficiently large, this division has been considered appropiate enough for our present work.

This set of best values of τ is consistent with those suggested recently by Vasyliunas [1987]. The three $|-Dst|$ domains (<50, 50-100, >100 nT), described in his Figure 1, suggest average values for τ similar to those given above. However, from the best values of τ, the one (4 hours) obtained for the lowest Dst domain ($\geq$-50 nT) is the least significative one, because most of the Dst values present during the selected intervals of our study were in the other two domains. Thus from an inspection of the τ variability influence in the correlation coefficients, values from 2 to 6 hours are practically also valid in this lower domain of Dst. However, in the other two domains, even exchanging 0.25 by 0.5 hours notably lowered the correlation coefficients.

The values of τ suggested by Burton et al. [1975], Feldstein et al. [1984] and Pudovkin et al. [1985], between 4 to 8 hours, are in our oppinion still valid for τ the main phase of moderate storms, in which Dst values $\geq$ -50 nT are more frequent because energy injection rates are expected to be smaller than during intense storms. For intense storms, such large values of τ seem inappropriate, as shown by the observed large decrease in the correlation coefficient values, and were found to lead to fairly low and insufficient energy injection rates, as discussed below. Furthermore, Burton et al. [1975] obtained their values of τ by asssuming $Q = 0$ in equation (1b), exactly for time intervals without energy injection. Thus their estimates seem more appropiate for the recovery phase of the storms.

It is important to point out that a variable behavior of τ was obtained under the assumption that the function Q of equation (1b) depends

solely on solar wind parameters, without any direct influence from magnetospheric parameters. Because the obtained correlation coefficients between Q and the other terms in equation (1b) were large enough, we conclude that this assumption is appropiate, at least for the most intense storms. However, more results using independent methods, which do not necessarily restrict the dependence of Q to solar wind parameters, besides those obtained by Vasyliunas [1987], are still needed for establishing a variable τ.

Ring Current Energization During Intense Storms

From the results shown in Table 5 one can get an idea of the average rate of energy injection to the ring current during intense storms. Using average Q values from <A>F and typical values of F for solar wind parameters during intense storms (Table 1), namely $N_H = 10\ cm^{-3}$, $V = 500\ km\ s^{-1}$, $B_z = -10\ nT$ and $B = 20\ nT$, the four best functions of Table 5 give injection energy rates of about $150 \pm 50\ nT(hour)^{-1}$. For larger values of the solar wind parameters, this injection rate can get values up to about 600 $nT(hour)^{-1}$ or more, although such conditions usually last for short time intervals <1 hour (at least during the studied events).

These injection rate values are considerably larger than those found by Burton et al. [1975] and Feldstein et al. [1984] for moderate storms. Their results suggest injection rate values of less than $30\ nT(hour)^{-1}$ for the same typical intense-storm solar wind values given above. This difference is explained mainly by the large difference in the values of used by them as compared to those found in our correlation studies. Although in principle such smaller injection rates and large τ values can still explain the growth of Dst values during intense storms, as discussed by Burton et al. [1975], they can not explain the Dst saturation at the peak Dst values of intense storms, which was observed to occur even when large values of negative B_z and V are still present. For instance, during the event of September 29, 1978 (Figure 2), the Dst growth got saturated at about -200 nT even when B_z fields of -20 nT and values of V of 800 km s^{-1} were still present. An estimate for an hourly change of Dst from expression (1b), with the injection rate and τ values suggested by Burton et al. [1975] and Feldstein et al. [1984], indicates that Dst should continue growing by about 60 nT or more in the following hour. On the other hand, the

larger injection rate and much smaller τ values suggested from our results, indicate a saturation regime, as observed.

However, for the earlier phase of Dst growth, especially for Dst >-100 nT, the results of Burton et al. [1975] and Feldstein et al. [1984] explain better than ours the observed Dst growth. Our results suggest a faster growth than observed (overestimation of the injection rates). This is explained by the fact that, in our correlation studies, the dominant Dst regime was that at <-120 nT. Thus an extension of our studies to moderate storms should be necessary in order to learn more about a possible transition between moderate to intense storms with respect to injection rate values.

Because the coupling function ϵ has been widely discussed in the literature and is one of the best functions found in our study, it is interesting to study how well this function satisfies known relationships involving the ring current. From Table 5, $Q=1.3\times10^{-17}\ \epsilon$ nT(hour)$^{-1}$. Thus using this in equation (1b) one gets:

$$\epsilon = 3\times10^{20}(d/dt + 1/\tau)D \qquad \text{ergs/s} \qquad (1c')$$

This expression is similar to expression (1c), obtained from (1a) and the Dessler-Parker-Sckopke relation. Thus ϵ seems to represent well the energy input, U_o, to the ring current, at least during intense storms. Since U_o has been also called U_t [Akasofu, 1981; Vasyliunas, 1987; Zwickl, 1987], then $\epsilon \sim U_t$ from (1c) and (1c'), as also found by Akasofu [1981] and Akasofu et al. [1985]. Furthermore, since τ has been found to depend on U_t [Vasyliunas, 1987], then equivalently, τ can also depend on ϵ [Akasofu, 1981], at least during intense storms.

Relationship of Best Coupling Functions to Interplanetary Features

As discussed above, all best coupling functions of Table 5 represent the reconnection power under one simplification or another [Gonzalez, 1988], aside from the stronger ram pressure modulation claimed during intervals with large pressure variations. Furthermore, from the solar wind parameters involved in these functions, it was observed that the main ingredient for the occurrence of intense storms (Dst < -100 nT) is the presence of large amplitude ($\leq$-10 nT) and long duration ($\geq$3 hours) negative B_z fields, together with values of

$V \geq 500$ km/s or, equivalently, of interplanetary dawn-dusk electric fields of ≥ 5 mV/m [Gonzalez and Tsurutani, 1987].

Therefore any interplanetary feature involving such B_z and V amplitude and duration values, regardeless of its type, is expected to produce an intense geomagnetic storm, with the required energy transmitted by large-scale reconnection.

Tsurutani et al., [1988] have identified the interplanetary features that caused the ten intense storms of our study. They are roughly the driver gas (four cases) or the sheath field (five cases) regions of interplanetary shocks, and high intensity draped fields (one case) without an interplanetary shock. Among those interplanetary features it appears that two involving sheath fields (March 29, 1979, and April 25, 1979) and one involving a driver gas (August 28, 1978) have the largest pressure variations among the ten studied events (Table 1). Thus as Table 3 shows, during such cases, functions with a stronger dependence on the pressure, such as $p^{1/2}VB_z$, seem to represent better the coupling.

Otherwise, it seems that there is not a particular function that better represents the coupling for each of the interplanetary features identified by Tsurutani et al. [1988]. However, a generalization of a conclusion of this sort is certainly premature before more events are studied.

5. Summary of Conclusions

From the present study the following conclusions can be drawn about ring current energization during intense storms:

Because the correlation coefficients obtained in the linear fit analysis are fairly large and all best coupling functions are related to magnetopause reconnection, one concludes that reconnection power can explain ring current energization and that there is no need to look for additional and significant energization mechanisms, at least during intense storms.

Among the tested coupling functions, the best and most common ones found in our study are ε, $p^{1/6}VB\sin^4(\theta/2)$, $p^{1/2}VB_z$ and the general function for large scale reconnection $P_D(s,\theta)$. Because the former functions are limits of $P_D(s,\theta)$, except for a ram pressure correction, this function is a candidate for a general representation of ring current energization, when the approximations presently used for its

computation are relaxed with better future knowledge of its composite parameters.

Events that involve large ram pressure variations seem to be better represented by functions with a stronger dependence on ram pressure, such as $p^{1/2}VB_z$. This function suggest that a correction, perhaps by the factor $p^{1/3} \propto L_{CF}^{-2}$, is necessary for reconnection-power models during intervals with large pressure variations.

The average time lag for transmission of the reconnection power from the magnetopause to the inner magnetosphere, during intense storms, is about 1 hour. There is an indication that this time lag decreases (increases) during more (less) intense events.

The AE response to the coupling functions shows large correlation coefficients during less intense storms and much smaller correlation coefficients during intense storms. This, together with the Dst response obtained in our study, suggest a decoupling between the ring current and auroral energization during intense storms from a direct solar wind influence.

The best set of τ values obtained in the correlation study was 4 hours for Dst $\geq$ -50 nT, 0.5 hours for -50 nT > Dst $\geq$ -120 nT, and 0.25 hours for Dst <-120 nT, in general agreement with recent and independent studies on this parameter.

A typical value for the ring current energy injection rate, during intense storms, was found to be 150 ± 50 nT(hour)$^{-1}$. This injection rate is considerably larger than values extrapolated from previous studies, restricted to moderate storms [Burton et al., 1975; Feldstein et al., 1984].

It is possible that interplanetary (shock related) sheath fields bring the largest ram pressure variations, for which a ram pressure modulation of the reconnection process seems to be important in order to represent better the coupling.

6. Final Remarks

Because the coupling functions used in this work depend solely on solar wind parameters, for the events with notably smaller correlation coefficients (Table 3) it is possible that internal magnetospheric parameters need to be also incorporated. This hypothesis, which belongs to the "driven-unloading" type of approach to magnetospheric energization research [e.g., Rostoker et al., 1987], should be tested when a quantitative knowledge of such internal magnetospheric parameters is obtained.

Appendix: Additional Functions

$p^{1/6}\ V\ B_z$
$p^{1/6}\ V\ B_T$
$p^{1/2}\ V\ B_T$
$p^{1/2}\ V\ B_z{}^{1/2}$
$p^{1/6}\ V\ B_z\ \sin(\theta/2)$
$p^{1/6}\ V\ B_T\ \sin(\theta/2)$
$p^{1/6}\ V\ B_T\ \sin^2(\theta/2)$
$p^{1/6}\ V\ B_z\ \sin^4(\theta/2)$
$p^{1/6}\ V\ B_T\ \sin^4(\theta/2)$
$p^{1/2}\ V\ B_z\ \sin(\theta/2)$
$p^{1/2}\ V\ B_T\ \sin(\theta/2)$
$p^{1/2}\ V\ B_z\ \sin^2(\theta/2)$
$p^{1/2}\ V\ B_z\ \sin^4(\theta/2)$
$p^{1/2}\ V\ B_z{}^2\ \sin^4(\theta/2)$
$p^{1/2}\ V\ B_T{}^{1/2}\ \sin(\theta/2)$
$p^{-1/3}\ V\ B^2\ \sin^2(\theta/2)$
$p^{-1/3}\ V\ B^2\ \sin^4(\theta/2)$

Appendix: Additional Functions

$p^{1/6}\ V\ B_z$

$p^{1/6}\ V\ B_T$

$p^{1/2}\ V\ B_T$

$p^{1/2}\ V\ B_z{}^{1/2}$

$p^{1/6}\ V\ B_z \sin(\theta/2)$

$p^{1/6}\ V\ B_T \sin(\theta/2)$

$p^{1/6}\ V\ B_T \sin^2(\theta/2)$

$p^{1/6}\ V\ B_z \sin^4(\theta/2)$

$p^{1/6}\ V\ B_T \sin^4(\theta/2)$

$p^{1/2}\ V\ B_z \sin(\theta/2)$

$p^{1/2}\ V\ B_T \sin(\theta/2)$

$p^{1/2}\ V\ B_z \sin^2(\theta/2)$

$p^{1/2}\ V\ B_z \sin^4(\theta/2)$

$p^{1/2}\ V\ B_z{}^2 \sin^4(\theta/2)$

$p^{1/2}\ V\ B_T{}^{1/2} \sin(\theta/2)$

$p^{-1/3}\ V\ B^2 \sin^2(\theta/2)$

$p^{-1/3}\ V\ B^2 \sin^4(\theta/2)$

Acknowledgements. This work was supported by the Fundo Nacional de Desenvolvimento Científico e Tecnológico under contract FINEP 537/CT and partially by a contract of the Jet Propulsion Laboratory, California Institute of Technology, with the National Aeronautics and Space Administration. We wish to thank S. J. Bame for the use of the Los Alamos ISEE 3 plasma data.

The editor thanks T. Murayama and R.D. Zwickl for their assistance in evaluating this paper.

References

Akasofu, S.-I., Energy coupling between the solar wind and the magnetosphere, Space Sci. Rev., 28, 111, 1981.

Akasofu, S.-I., Some critical issues on magnetospheric substorms, Planet. Space Sci., 34, 563, 1986.

Akasofu, S.-I., C. Olmsted, E. J. Smith, B. T. Tsurutani, R. Okida, and D. N. Baker, Solar wind variations and geomagnetic storms: A study of individual storms based on high time resolution ISEE 3 data, J. Geophys. Res., 90, 325, 1985.

Baker, D. N., Statistical analysis in the study of solar wind-magnetosphere coupling, in Solar Wind-Magnetosphere Coupling, Edited by Y. Kamide and J. A. Slavin, pp. 17-38, Terra, Tokyo, Japan, 1986.

Baker, D. N., R. D. Zwickl, S. J. Bame, E. W. Hones, Jr., B. T. Tsurutani, E. J. Smith, and S.-I. Akasofu, An ISEE 3 high time resolution study of interplanetary parameter correlations with magnetic activity, J. Geophys. Res., 88, 6230, 1983.

Bame, S. J., J. R. Asbridge, H. E. Felthauser, J. P. Gore, H. L. Hawk, and J. Chaves, ISEE-C solar wind plasma experiment, IEEE Trans. Geosci. Electron., GE-16, 160, 1978.

Bargatze, L. F., D. N. Baker, and R. L. McPherron, Solar wind-magnetosphere energy input functions, in Solar Wind-Magnetosphere Coupling, Edited by Y. Kamide and J.A.Slavin, pp. 101-109, Terra, Tokyo, Japan, 1986.

Burton, R. K., R. L. McPherron, and C. T. Russell, An empirical relationship between interplanetary conditions and Dst, J. Geophys. Res., 80, 4204, 1975.

Clauer, C. R., The technique of linear prediction filters applied to studies of solar wind-magnetosphere coupling, in Solar Wind Magnetosphere Coupling, Edited by Y. Kamide and J. A. Slavin, pp. 39-57, Terra, Tokyo, Japan, 1986.

Crooker, N. U., G. L. Siscoe, P. R. Mullen, C. T. Russell, and E. J. Smith, Magnetic field compression at the dayside magnetosphere, J. Geophys. Res., 87, 10, 407, 1982.

Fay, R. A., C. R. Garrity, R. L. McPherron, and L. F. Bargatze, Prediction filters for the Dst index and the polar cap potential, in Solar Wind-Magnetosphere Coupling, Edited by Y. Kamide and J. A. Slavin, pp. 111-118, Terra, Japan, 1986.

Feldstein, Y. J., V. Yu. Pisarsky, N. M. Rudneva, and A. Grafe, Ring current simulation in connection with interplanetary space conditions, Planet. Space Sci., 32, 975, 1984.

Frandsen, A. M. A., B. V. Connor, J. Vam Amersfoort, and E. J. Smith, The ISEE-C vector helium magnetometer. IEEE Trans. Geosci. Electron., GE-16, 195, 1978.

Gonzalez, W. D., Electric field and energy transfer by magnetopause reconnection, in Solar Wind-Magnetosphere Coupling, Edited by Y. Kamide and J. A. Slavin, pp. 315-320, Terra,, Tokyo, Japan, 1986.

Gonzalez, W. D., Solar wind-magnetosphere coupling functions and large scale magnetopause reconnection, INPE, 4676-PRE/1373, São José dos Campos, São Paulo, Brazil, 1988.

Gonzalez, W. D., and A. L. C. Gonzalez, Solar wind energy and electric field transfer to the Earth's via magnetopause reconnection, Geophys. Res. Lett., 8, 265, 1981.

Gonzalez, W. D., and A. L. C. Gonzalez, Energy transfer by magnetopause reconnection and the substorms parameter ε, Planet. Space Sci., 32, 1007, 1984.

Gonzalez, W. D., and F. S. Mozer, A quantitative model for the potential resulting from reconnection with an arbitrary interplanetary magnetic field, J. Geophys. Res., 79, 4186, 1974.

Gonzalez, W. D., and B. T. Tsurutani, Criteria of interplanetary parameters causing intense magnetic storms (Dst <-100 nT), Planet. Space Sci., 35, 1101, 1987.

Gonzalez, W. D., A. L. C. Gonzalez, and B. T. Tsurutani, Comments on "Large scale response of the magnetosphere to a southward turning of the interplanetary magnetic field" by J. A. Sauvant et al., J. Geophys. Res., in press, 1989.

Gosling, J. T., E. Hildner, J. R. Asbridge, S. J. Bame, and W. C. Feldman, Noncompressive density enhancements in the solar wind, J. Geophys. Res., 82, 5005, 1977.

Iyemori, T., H. Maeda, and T. Kamei, Impulse response of geomagnetic indices to interplanetary magnetic fields, J. Geophys. Res., 31, 1, 1979.

Kan, J. R., and L. C. Lee, Energy coupling functions and solar wind-magnetosphere dynamo, Geophys. Res. Lett., 6, 577, 1979.

Kelly, T. J., N. U. Crooker, G. L. Siscoe, C. T. Russell, and E. J. Smith, On the use of a sunward libration-point-orbiting spacecraft as an interplanetary magnetic field monitor for magnetospheric studies, J. Geophys. Res., 91, 5629, 1986.

Maezawa, K., and T. Murayama, Solar wind velocity effects on the auroral zone magnetic disturbances, in Solar Wind Magnetosphere Coupling, Edited by Y. Kamide and J. A. Slavin, pp. 59-84, Terra, Tokyo, Japan, 1986,

Murayama, T., Coupling function between solar wind parameters and geomagnetic indices, Rev. Geophys., 20, 623, 1982.

Murayama, T., Coupling functions between solar wind and the Dst index, in Solar Wind Magnetosphere Coupling, Edited by Y.Kamide and J. A. Slavin, pp. 119-126, Terra, Tokyo, Japan, 1986.

Perreault, P., and S.-I. Akasofu, A study of geomagnetic storms, Geophys. J. R. Astron. Soc., 54, 547, 1978.

Pudovkin, M. I., S. A. Zaitseva, and L. Z. Sizova, Growth rate and decay of magnetospheric ring current, Planet. Space Sci., 33, 1097, 1985.

Rostoker, G., S.-I. Akasofu, W. Baumjohann, Y. Kamide, and R. McPherron, The roles of direct imput of energy from the solar wind and unloading of stored magnetotail energy in driven magnetospheric substorms, Space Sci. Rev., 46, 93, 1987.

Sckopke, N., A general relation between the energy of trapped particles and the disturbance field near the Earth, J. Geophys. Res., 71, 3125, 1966.

Smith, E. J., J. A. Slavin, R. D. Zwickl, and S. J. Bame, Shocks and storm sudden commencements, in Solar Wind Magnetosphere Coupling, Edited by Y. Kamide and J. A. Slavin, pp. 345-365, Terra, Tokyo, Japan, 1986.

Tang, F., B. T. Tsurutani, W. D. Gonzalez, S.-I. Akasofu, and E. J. Smith, Solar sources of interplanetary southward B events responsible for major magnetic storms (1978-1979), J. Geophys. Res., in press, 1989.

Tsurutani, B. T., J. A. Slavin, Y Kamide, R. D. Zwickl, J. H. King, and C. T. Russell, Coupling between the solar wind and the magnetosphere: CDAW 6, J. Geophys. Res., 90, 1191, 1985.

Tsurutani, B. T., W. D. Gonzalez, F. Tang, S.-I. Akasofu, and E. J. Smith, Origin of interplanetary southward magnetic fields responsible for major magnetic storms near solar maximum (1978-1979), J. Geophys. Res., 93, 8519, 1988.

Vasyliunas, V. M., A method for evaluating the total magnetospheric energy output independently of the ε parameter, Geophys. Res. Lett., 14, 1183, 1987.

Vasyliunas, V. M., J. R. Kan, G. L. Siscoe, and S.-I. Akasofu, Scaling relations governing magnetospheric energy transfer, Planet. Space Sci., 30, 359, 1982.

Zwickl, R. D., L. F. Bargatze, D. N. Baker, C. R. Clauer, and R. L. McPherron, An evalutaion of the total magnetospheric energy output parameter, U , in Magnetotail Physics, edited by A. T. Lui, pp. 155-159, Johns Hopkins University Press, Baltimore, Md., 1987.

S.-I. Akasofu, Geophysical Institute, University of Alaska, Fairbanks, AK 99775.

A.L.C. Gonzalez, and W.D. Gonzalez, Instituto de Pesquisas Espaciais (INPE), Caixa Postal 515, 12201, São José dos Campos, São Paulo, Brazil.

E.J. Smith, and B.T. Tsurutani, Jet Propulsion Laboratory, 4800 Dok Grove Drive, Pasadena, CA 91109.

F. Tang, California Institute of Technology, Pasadena, CA 91125.

(Received July 27, 1988;
revised December 14, 1988;
accepted January 9, 1989).

Paper number 89JA00059.
0148-0227/89/89JA-0005$05.00

Gonzalez et al.: Solar Wind-Magnetosphere Coupling
Gonzalez et al.: Solar Wind-Magnetosphere Coupling
Gonzalez et al.: Solar Wind-Magnetosphere Coupling
Gonzalez et al.: Solar Wind-Magnetosphere Coupling
Gonzalez et al.: Solar Wind-Magnetosphere Coupling
Gonzalez et al.: Solar Wind-Magnetosphere Coupling
Gonzalez et al.: Solar Wind-Magnetosphere Coupling
Gonzalez et al.: Solar Wind-Magnetosphere Coupling
Gonzalez et al.: Solar Wind-Magnetosphere Coupling
Gonzalez et al.: Solar Wind-Magnetosphere Coupling
Gonzalez et al.: Solar Wind-Magnetosphere Coupling
Gonzalez et al.: Solar Wind-Magnetosphere Coupling
Gonzalez et al.: Solar Wind-Magnetosphere Coupling
Gonzalez et al.: Solar Wind-Magnetosphere Coupling
Gonzalez et al.: Solar Wind-Magnetosphere Coupling
Gonzalez et al.: Solar Wind-Magnetosphere Coupling
Gonzalez et al.: Solar Wind-Magnetosphere Coupling
Gonzalez et al.: Solar Wind-Magnetosphere Coupling
Gonzalez et al.: Solar Wind-Magnetosphere Coupling
Gonzalez et al.: Solar Wind-Magnetosphere Coupling
Gonzalez et al.: Solar Wind-Magnetosphere Coupling
Gonzalez et al.: Solar Wind-Magnetosphere Coupling
Gonzalez et al.: Solar Wind-Magnetosphere Coupling
Gonzalez et al.: Solar Wind-Magnetosphere Coupling
Gonzalez et al.: Solar Wind-Magnetosphere Coupling
Gonzalez et al.: Solar Wind-Magnetosphere Coupling
Gonzalez et al.: Solar Wind-Magnetosphere Coupling

[1]INPE, São José dos Campos, São Paulo, Brazil.
[2]Jet Propulsion Laboratory, Pasadena, California.
[3]California Institute of Technology, Pasadena, California.
[4]Geophysical Institute, University of Alaska, Fairbanks.

Fig. 1. Overview of the ten intense magnetic storms and associated interplanetary phenomena. Taken from Gonzalez and Tsurutani [1987]. From left to right are the interplanetary phenomena detected prior to the large southward IMF events causing the intense storms (Mach number, if shocks), peak southward B_z, peak IMF magnitudes, and peak Dst. Nine storm events had leading interplanetary shocks, and one had a leading noncompressive density enhancement event.

Fig. 2. Interplanetary field and plasma data for September 28-29, 1978, including the intense storm event of September 29, 1978, with a peak Dst value of -215 nT at about 1100 UT. The letter S in the B panel indicates the passage of an interplanetary shock. In this figure, as in Figures 3 and 4, Dst is not pressure corrected.

Fig. 3. Interplanetary field and plasma data for November 24-25, 1978, including the intense storm event on November 25, 1978, with a peak Dst value of -150 nT at about 1900 UT. The letter S in the B panel indicates the passage of an interplanetary shock.

Fig. 4. Interplanetary field and plasma data for September 17-18, 1979, including the intense storm event of September 18, 1979, with a peak Dst value of -150 nT at about 1700 UT. The storm main phase was studied only partially during the interval 0000 UT to 0800 UT due to the data gap.

Fig. 5. Exponent of the ram pressure factor p in the best coupling functions, given in Table 3, as a function of the corresponding relative ram pressure variability, given in the last column of Table 1, for each of the studied events. See text for explanation of the cross and dot marks.

Table 1. Summary of Some Important Features for the Intense Storm Events

Event	ΔT of Dst growth, UT hours	Peak Dst, nT	$\langle B_z \rangle$, nT	$\langle V \rangle$, $km.s^{-1}$	$\langle p \rangle$, $eV.cm^{-3} \times 10^3$
Aug. 28, 1978	0000-1000	-220	-15 (±5)	450 (±25)	24 (±15)
Sept. 29, 1978	0700-1100	-215	-20 (±5)	850 (±50)	36 (±15)
Nov. 25, 1978	1300-1900	-150	-14 (±3)	475 (±10)	35 (±10)
Feb. 21, 1979	0500-0900+	-100	-7 (±6)	475 (±15)	34 (± 7)
	1700-2200	-110	-9 (±4)	525 (±15)	65 (±20)
March 10, 1979	1800-2400	-140	-11 (±4)	450 (±25)	20 (± 6)
March 29, 1979	0500-0900+	-100	-7 (±3)	550 (±25)	15 (± 9)
	1200-2200	-120	-8 (±4)	500 (±25)	13 (± 6)
April 3, 1979	1600-2400	-200	-13 (±4)	550 (±25)	30 (± 6)
April 25, 1979	1200-1800*	-140	-4 (±3)	620 (±50)	40 (±30)
Aug. 29, 1979	0900-1900	-140	-8 (±4)	520 (±30)	28 (± 7)
Sept. 18, 1979	0000-0800*	-150	-3 (±7)	420 (±15)	40 (±15)

$\langle B_z \rangle$, $\langle V \rangle$ and $\langle p \rangle$ indicate average estimates, given with their range of variability values, for the selected time intervals shown in column 2.

Table 2. List of Tested Coupling Functions

	Function
E	$V\ B_z$
	$V\ B_T \sin^2(\theta/2)$
ϵ	$V\ B^2 \sin^4(\theta/2)$
	$p^{1/6}\ V\ B \sin^4(\theta/2)$
P	$p^{1/2}\ V\ B_z$
	$p^{1/2}\ V\ B_T{}^{1/2}$
R	$p^{-1/3}\ V\ B_T\ B_M\ K(s,\theta)$

Given in the Text.

Table 3. Best Coupling Functions, for Each of the Intense Storm Events, Together With Their Correlation Coefficients, Time Lags, and Best Set of τ Values

Event		Best Coupling Functions	Correlation Coefficients	Lag, min	Best Set of τ Values
Aug. 28, 1978	P'	$p^{1/2}VB_z{}^{1/2}$	0.98	55	(4,0.5,0,25)
0000-1000 UT	P'	$p^{1/2}VB_z \sin(\theta/2)$	0.97	60	(4,0.5,0,25)
	P		0.97	45	(4,0.5,0,25)
	E'	$p^{1/6}VB_T \sin^4(\theta/2)$	0.95	75	(4,0.5,0,25)
	R		0.93	75	(4,0.5,0,25)
Sept. 29. 1979	E'	$p^{1/6}VB \sin^4(\theta/2)$	0.92	35	(4,0.5,0,25)
0070-1100 UT	ϵ		0.91	30	(4,0.5,0,25)
	P		0.85	40	(4,0.5,0,25)
	R		0.84	40	(4,0.5,0,25)
Nov. 25, 1978	E'	$p^{1/6}VB_T$	0.91	60	(4,0.5,0.5)
1300-1900 UT	P'	$p^{1/2}VB_T$	0.90	60	(4,0.5,0.5)
	R		0.88	65	(4,0.5,0.5)
	P		0.86	60	(4,0.5,0.5)
	E'	$p^{1/6}VB \sin^4(\theta/2)$	0.85	60	(4,0.5,0.5)
Feb. 21, 1979	E		0.77	130	(4,0.5)
1700-2200 UT	ϵ'	$p^{-1/3}VB^2 \sin^4(\theta/2)$	0.77	155	(4,0.5)
	ϵ		0.76	145	(4,0.5)
	P		0.75	120	(4,0.5)
0500-0900 UT	ϵ		0.67	35	(4,0.5)
	E'	$p^{1/6}VB \sin^4(\theta/2)$	0.63	35	(4,0.5)
March 10, 1979	E		0.95	135	(4,0.5,0,5)
1800-2400 UT	E'	$p^{1/6}VB_T \sin^4(\theta/2)$	0.94	140	(4,0.5,0,5)
	ϵ		0.93	140	(4,0.5,0,5)
	R		0.93	140	(4,0.5,0,5)
	E'	$p^{1/6}VB \sin^4(\theta/2)$	0.92	140	(4,0.5,0,5)
March 29, 1978	P'	$p^{1/2}VB_z{}^2 \sin^4(\theta/2)$	0.83	50	(4,0.5)
0500-0900 UT	P		0.79	50	(4,0.5)
	E'	$p^{1/6}VB_z \sin^4(\theta/2)$	0.78	65	(4,0.5)
	ϵ		0.77	95	(4,0.5)
	R		0.77	55	(4,0.5)
1200-2200 UT	P		0.57	90	(4,0.5,0.25)
	P'	$p^{1/2}VB_z \sin(\theta/2)$	0.57	90	(4,0.5,0.25)
April 3, 1979	ϵ		0.91	30	(4,0.5,0,25)
1600-2400 UT	R		0.88	0	(4,0.5,0,25)
	E'	$p^{1/6}VB \sin^4(\theta/2)$	0.87	0	(4,0.5,0,25)
April 25, 1979	P'	$p^{1/2}VB_z{}^{1/2}$	0.77	185	(4,0.5,0,25)
1200-1800 UT	ϵ'	$p^{-1/3}VB^2 \sin^2(\theta/2)$	0.77	115	(4,0.5,0,25)
	P		0.72	185	(4,0.5,0,25)
Aug. 29, 1979	E'	$p^{1/6}VB_T \sin(\theta/2)$	0.57	90	(4,0.25,0.25)
0900-1900 UT	P'	$p^{1/2}VB_T{}^{1/2} \sin(\theta/2)$	0.55	140	(4,0.25,0.25)
Sept. 18, 1979	E'	$p^{1/6}VB_T$	0.59	30	(4,0.25,0.25)
0000-0800 UT	P'	$p^{1/2}VB_T$	0.57	35	(4,0.25,0.25)

Table 4. Summary of the Best Coupling Functions for the AE Response During the Same Time Intervals Selected for Study of Intense Storm Events

Event		Best Coupling Function for AE	Correlation Coefficient	Lag, Min
Aug. 28, 1978 0000-1000 UT			<0.40	
Sept. 29, 1978 0700-1100 UT			<0.40	
Nov. 25, 1978 1300-1900 UT			<0.30	
Feb. 21, 1979 0500-0900 UT	E'	$p^{1/2}VB \sin^4(\theta/2)$	0.80	10
1700-2200 UT	E		0.85	20
	P		0.82	15
	R		0.77	20
March 10, 1979 1800-2400 UT			<0.30	
March 29, 1979 0500-0900 UT	ϵ'	$p^{-1/3}VB^2 \sin^2(\theta/2)$	0.91	45
1200-2200 UT			<0.40	
April 3, 1979 1600-2400 UT			<0.30	
April 25, 1979 1200-1800 UT	E'	$p^{1/6}VB \sin^4(\theta/2)$	0.61	20
	ϵ		0.61	20
Aug. 29, 1979 0900-1900 UT			<0.40	
Sept. 18, 1979 0000-0800 UT	P'	$p^{1/2}VB_z^{1/2}$	0.88	45
	E		0.88	50

Their correlation coefficients and time lags are also given.

Table 5. Summary of the Best and Most Common Coupling Functions Found for the Intense Storm Events

Best and Most Common Coupling Function (F)		Number of Events Present	Lag, Min	Most Common Set of τ Values, Hours	Coupling Constant <A>, (nT/Hour) x (units of F)$^{-1}$
R	$p^{-1/3}VB_TB_MK(s,\theta)$	6	67 (±45)	(4,0.5,0.25)	(3.2±1.5) F in Gaussian units
ε	$VL_o^2B^2\sin^4(\theta/2)$	6	56 (±43)	(4,0.5,0.25)	(1.3±0.6) x 10^{-1} F in Gaussian units
P	$p^{1/2}VB_z$	6	70 (±60)	(4,0.5,0.25)	(0.6±0.4) x 10^9 F in MKS units
E'	$p^{1/6}VB\sin^4(\theta/2)$	5	48 (±51)	(4;0.5,0.25)	(1.0±0.2) x 10^6 F in MKS units

The number of events in which they are present, average time lag, most common se of τ values and average coupling constant <A> are also given. Averages are give with their standard deviations.

Table 6. Correlation Coefficients for the Four Coupling Functions Shown in Table 5 for Each of the Twelve Studied Events

Event	R	ε	P	E'
Aug. 28, 1978	**0.93**	0.72	**0.97**	0.92
Sept. 29, 1978	**0.84**	**0.91**	**0.85**	**0.92**
Nov. 25, 1978	0.88	0.84	0.86	0.85
Feb. 21, 1979 (1st. event)	0.56	**0.76**	**0.75**	0.72
Feb. 21, 1979 (2nd. event)		**0.67**	0.42	**0.63**
March 10, 1979	**0.93**	**0.93**	0.88	**0.92**
March 29, 1979 (1st event)	**0.77**	**0.77**	**0.79**	0.74
March 29, 1979 (2nd event)	0.47	0.45	0.57	0.48
April 3, 1979	**0.88**	**0.91**	0.81	**0.87**
April 25, 1979	0.55	0.59	**0.72**	0.57
Aug. 29, 1979	0.44	0.38	...	0.45
Sept. 18, 1979	0.37	0.44	0.53	0.38

The numbers in boldface are those that also appear on Table 3 and have been used for the information shown in column 2 of Table 5.

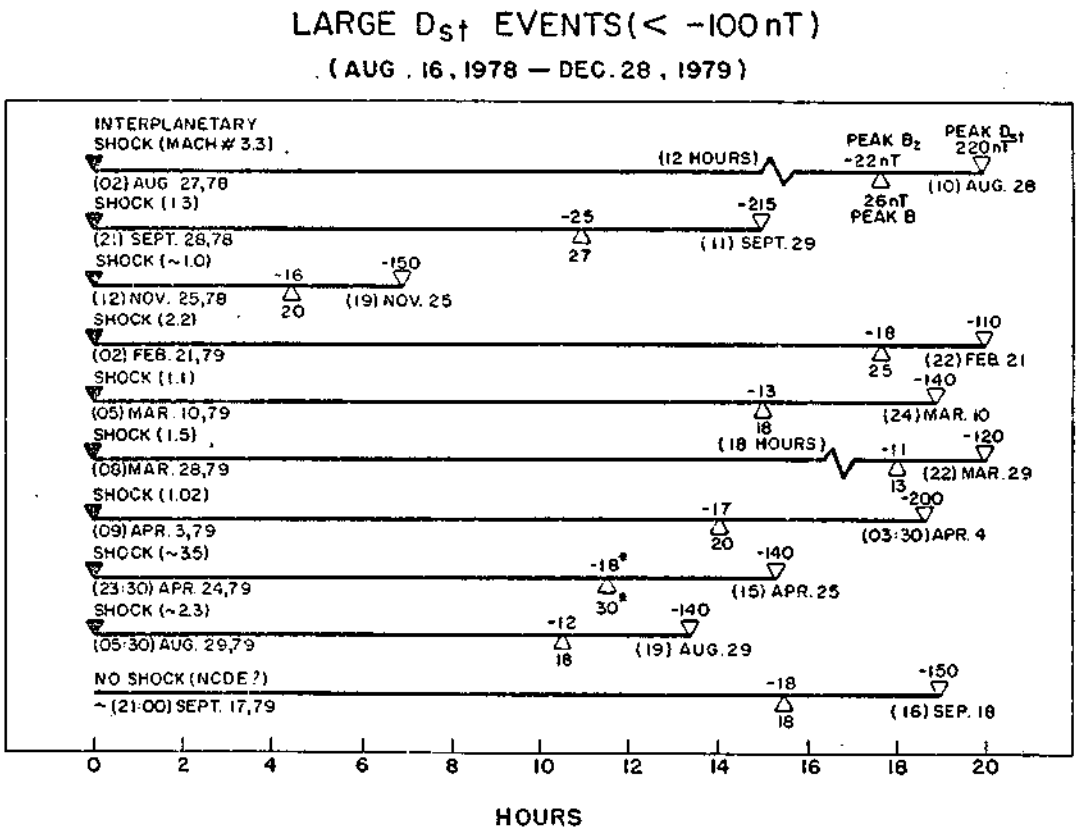
LARGE D_{st} EVENTS(< -100nT)
(AUG. 16, 1978 — DEC. 28, 1979)
INTERPLANETARY
SHOCK (MACH # 3.3)
(12 HOURS)
PEAK B_z
-22nT
PEAK D_{st}
220nT
(02) AUG 27,78
SHOCK (1.3)
-25
-215
26nT
PEAK B
(10) AUG. 28
(21) SEPT. 28,78
27
(11) SEPT. 29
SHOCK (~1.0)
-16
-150
(12) NOV. 25,78
20
(19) NOV. 25
SHOCK (2.2)
-18
-110
(02) FEB. 21,79
25
(22) FEB. 21
SHOCK (1.1)
-140
-13
(05) MAR. 10,79
18
(24) MAR. 10
SHOCK (1.5)
(18 HOURS)
-11
-120
(08) MAR. 28,79
13
(22) MAR. 29
SHOCK (1.02)
-200
-17
(09) APR. 3,79
20
(03:30) APR. 4
SHOCK (~3.5)
-140
-18*
(23:30) APR. 24,79
30*
(15) APR. 25
SHOCK (~2.3)
-140
-12
(05:30) AUG. 29,79
18
(19) AUG. 29
NO SHOCK (NCDE?)
-18
-150
~(21:00) SEPT. 17,79
18
(16) SEP. 18
0
2
4
6
8
10
12
14
16
18
20
HOURS

Fig. 1

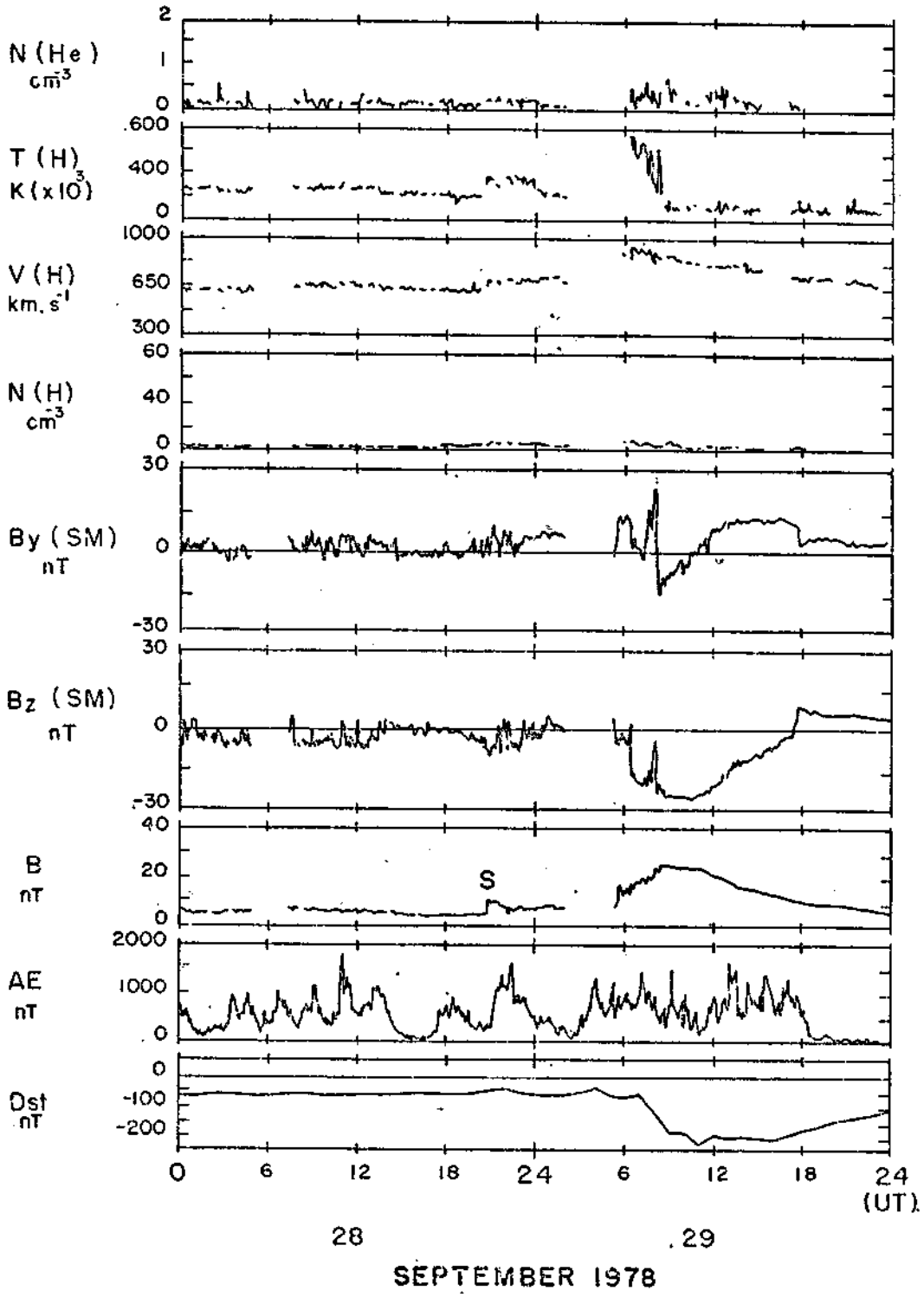
N (He)
cm⁻³
2
1
0
T (H)
K (x10³)
600
400
0
V (H)
km. s⁻¹
1000
650
300
N (H)
cm⁻³
60
40
0
By (SM)
nT
30
0
-30
Bz (SM)
nT
30
0
-30
B
nT
40
20
0
S
AE
nT
2000
1000
0
Dst
nT
0
-100
-200
0
6
12
18
24
6
12
18
24
(UT)
28
29
SEPTEMBER 1978

Fig. 2

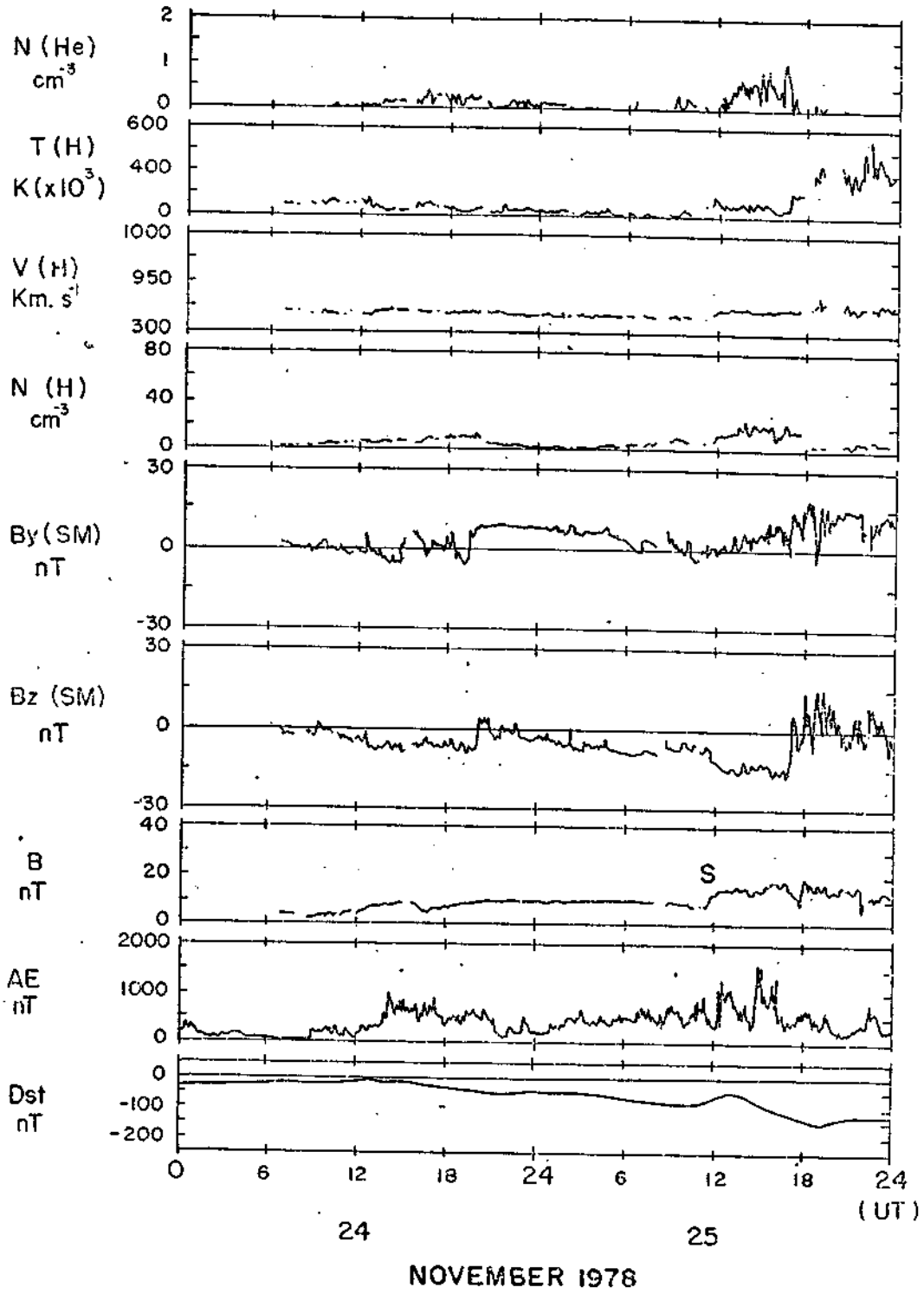
N (He)
cm-3
2
1
0
T (H)
K (x10^3)
600
400
0
V (H)
Km. s-1
1000
950
300
N (H)
cm-3
80
40
0
By (SM)
nT
30
0
-30
Bz (SM)
nT
30
0
-30
B
nT
40
20
0
S
AE
nT
2000
1000
0
Dst
nT
0
-100
-200
0
6
12
18
24
6
12
18
24
(UT)
24
25
NOVEMBER 1978

Fig. 3

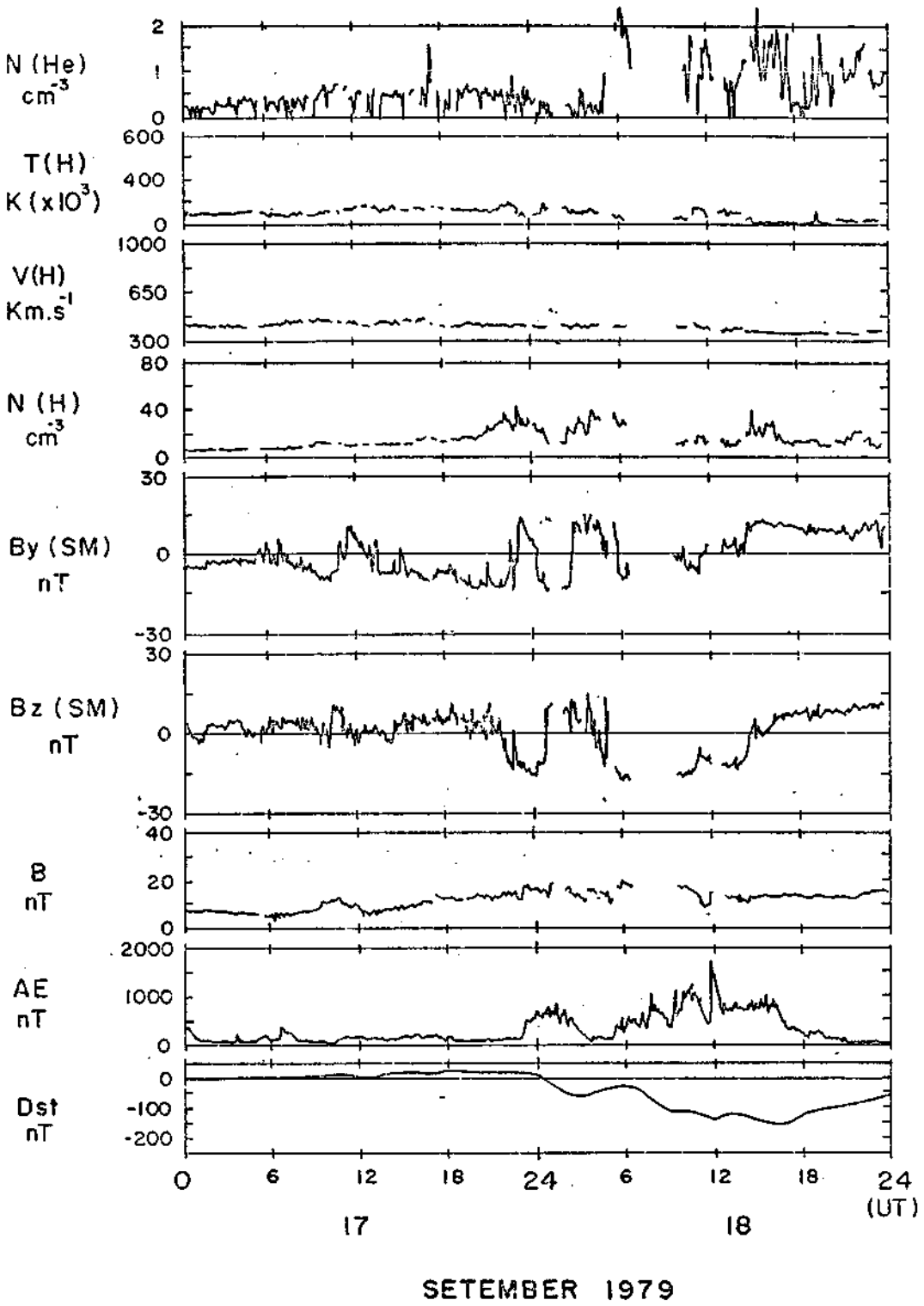
N (He)
cm-3
2
1
0
T(H)
K (x10^3)
600
400
0
V(H)
Km.s-1
1000
650
300
N (H)
cm-3
80
40
0
By (SM)
nT
30
0
-30
Bz (SM)
nT
30
0
-30
B
nT
40
20
0
AE
nT
2000
1000
0
Dst
nT
0
-100
-200
0
6
12
18
24
6
12
18
24
(UT)
17
18
SETEMBER 1979

Fig. 4

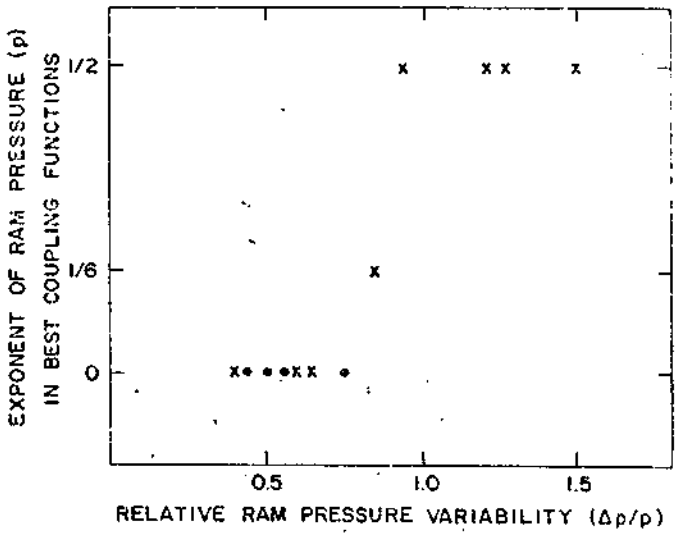
EXPONENT OF RAM PRESSURE (p)
IN BEST COUPLING FUNCTIONS
1/2
1/6
0
0.5
1.0
1.5
RELATIVE RAM PRESSURE VARIABILITY (Δp/p)

Fig. 5

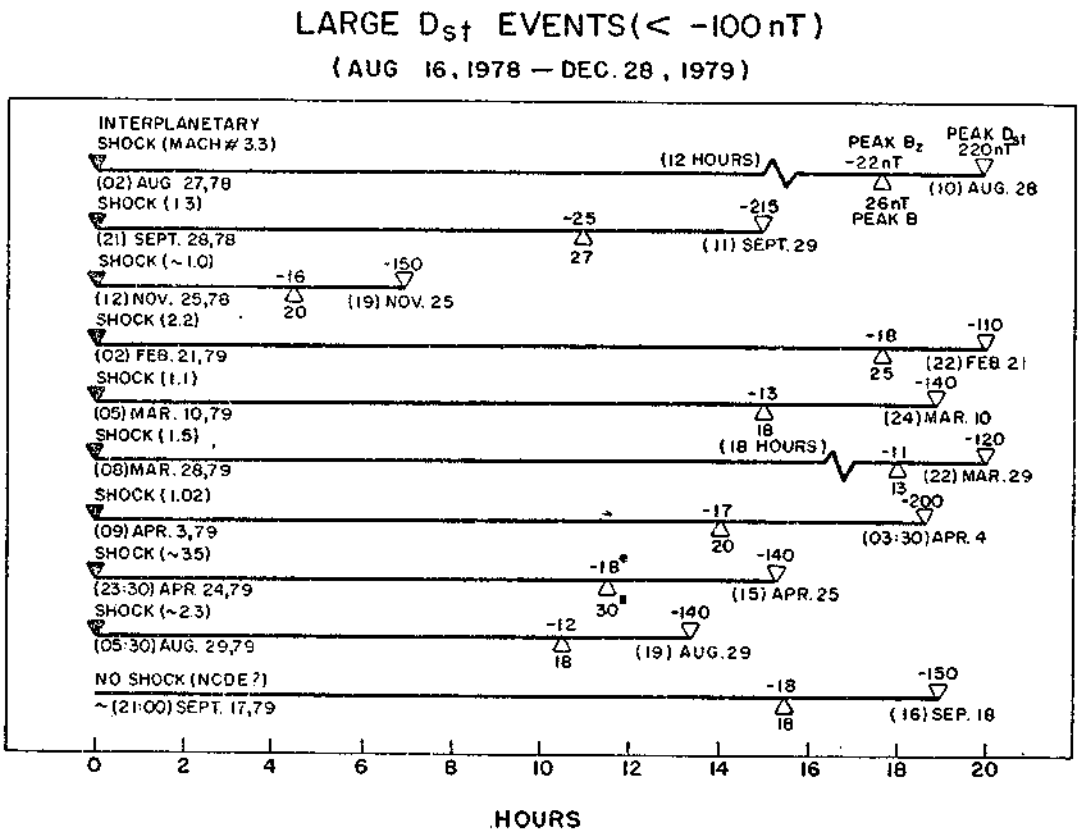
LARGE D_{st} EVENTS(< -100 nT)
(AUG 16, 1978 — DEC. 28, 1979)
INTERPLANETARY
SHOCK (MACH # 3.3)
(02) AUG 27,78
SHOCK (1.3)
(21) SEPT. 28,78
SHOCK (~1.0)
(12) NOV. 25,78
SHOCK (2.2)
(02) FEB. 21,79
SHOCK (1.1)
(05) MAR. 10,79
SHOCK (1.5)
(08) MAR. 28,79
SHOCK (1.02)
(09) APR. 3,79
SHOCK (~3.5)
(23:30) APR. 24,79
SHOCK (~2.3)
(05:30) AUG. 29,79
NO SHOCK (NODE?)
~(21:00) SEPT. 17,79
(12 HOURS)
PEAK B_z
-22 nT
PEAK D_{st}
220 nT
(10) AUG. 28
26 nT
PEAK B
-25
27
-215
(11) SEPT. 29
-16
20
-150
(19) NOV. 25
-18
25
-110
(22) FEB 21
-13
18
-140
(24) MAR. 10
(18 HOURS)
-11
13
-120
(22) MAR. 29
-17
20
-200
(03:30) APR. 4
-18*
30
-140
(15) APR. 25
-12
18
-140
(19) AUG. 29
-18
18
-150
(16) SEP. 18
0
2
4
6
8
10
12
14
16
18
20
HOURS

Fig. 1

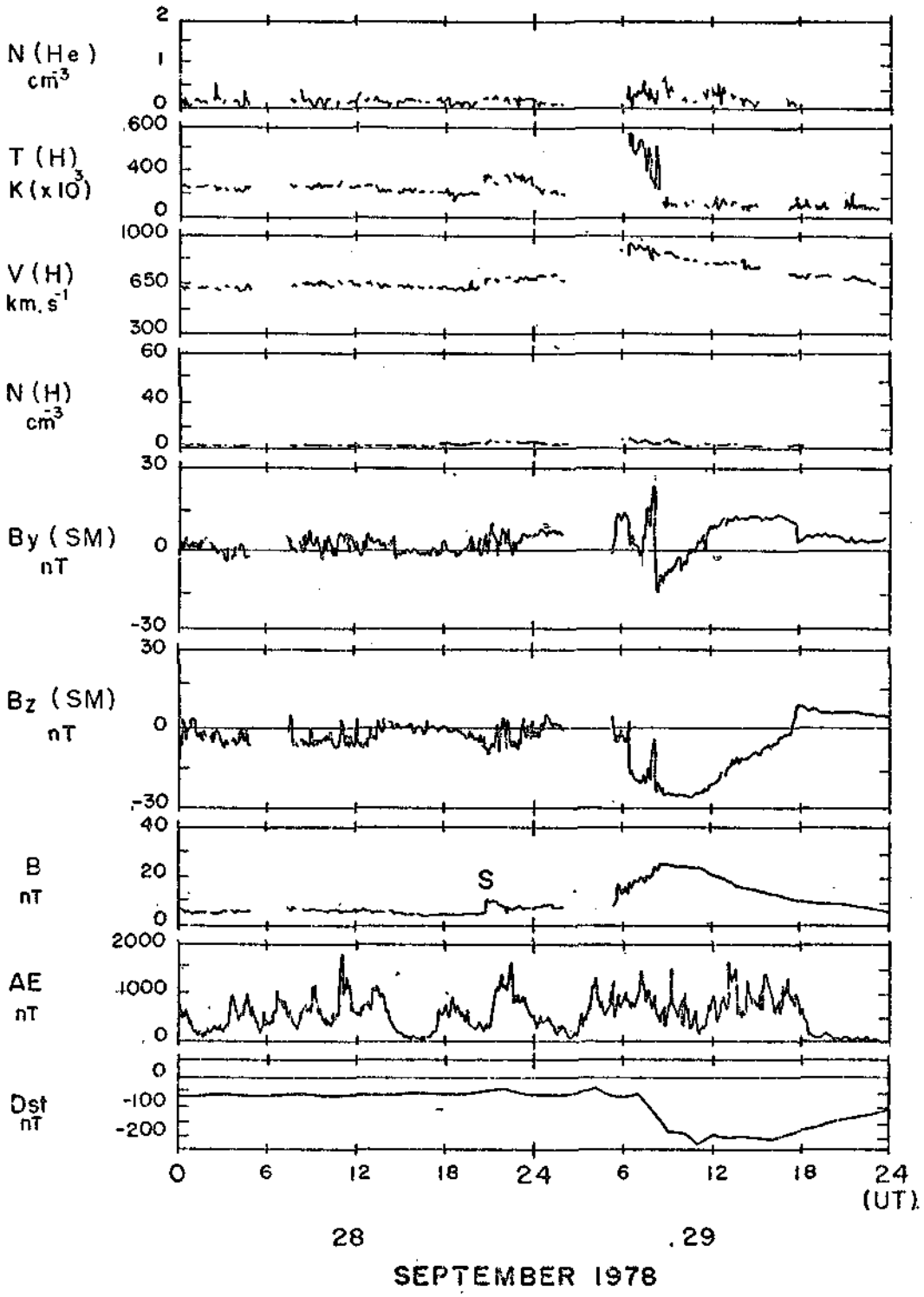
N (He)
cm-3
2
1
0
T (H)
K (x 10)3
600
400
0
V (H)
km. s-1
1000
650
300
N (H)
cm-3
60
40
0
By (SM)
nT
30
0
-30
Bz (SM)
nT
30
0
-30
B
nT
40
20
0
S
AE
nT
2000
1000
0
Dst
nT
0
-100
-200
0
6
12
18
24
6
12
18
24
(UT)
28
29
SEPTEMBER 1978

Fig. 2

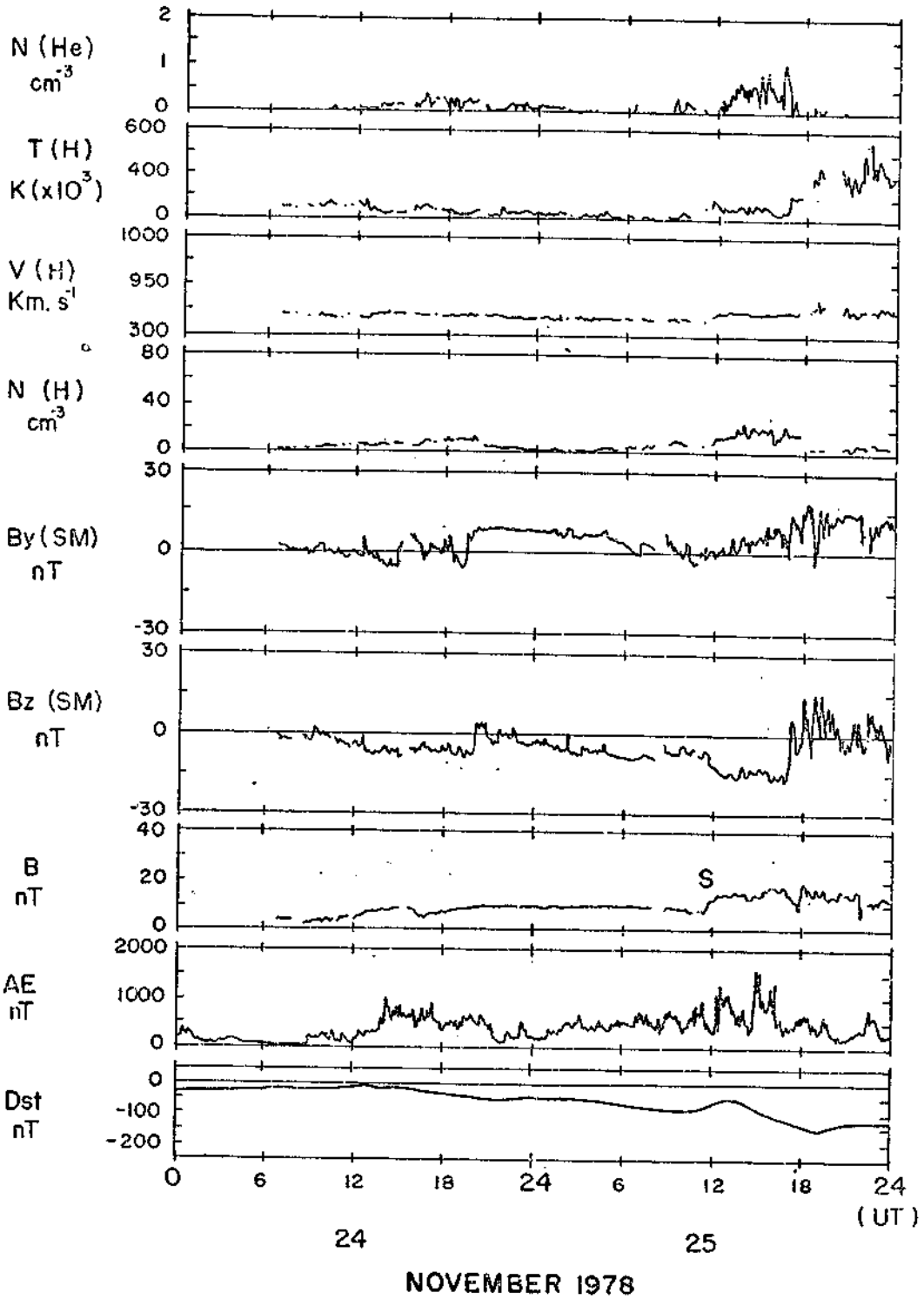
N (He)
cm-3
2
1
0
T (H)
K (x10^3)
600
400
0
V (H)
Km. s-1
1000
950
300
N (H)
cm-3
80
40
0
By (SM)
nT
30
0
-30
Bz (SM)
nT
30
0
-30
B
nT
40
20
0
S
AE
nT
2000
1000
0
Dst
nT
0
-100
-200
0
6
12
18
24
6
12
18
24
(UT)
24
25
NOVEMBER 1978

Fig. 3

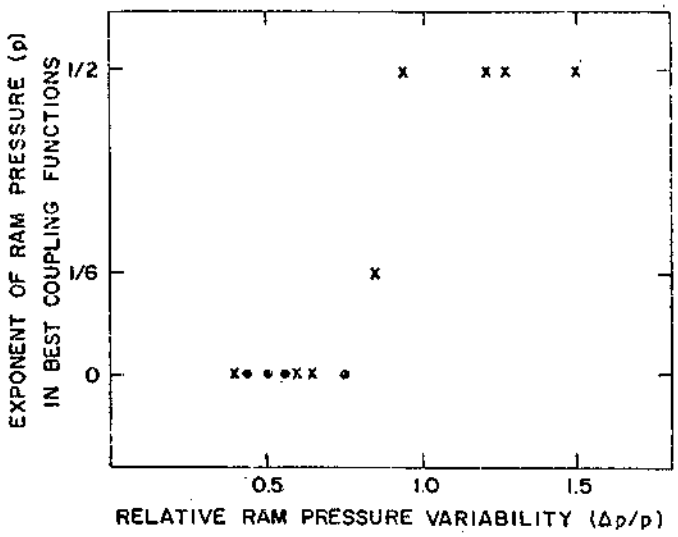
EXPONENT OF RAM PRESSURE (p)
IN BEST COUPLING FUNCTIONS
1/2
1/6
0
0.5
1.0
1.5
RELATIVE RAM PRESSURE VARIABILITY (Δp/p)

Fig. 5

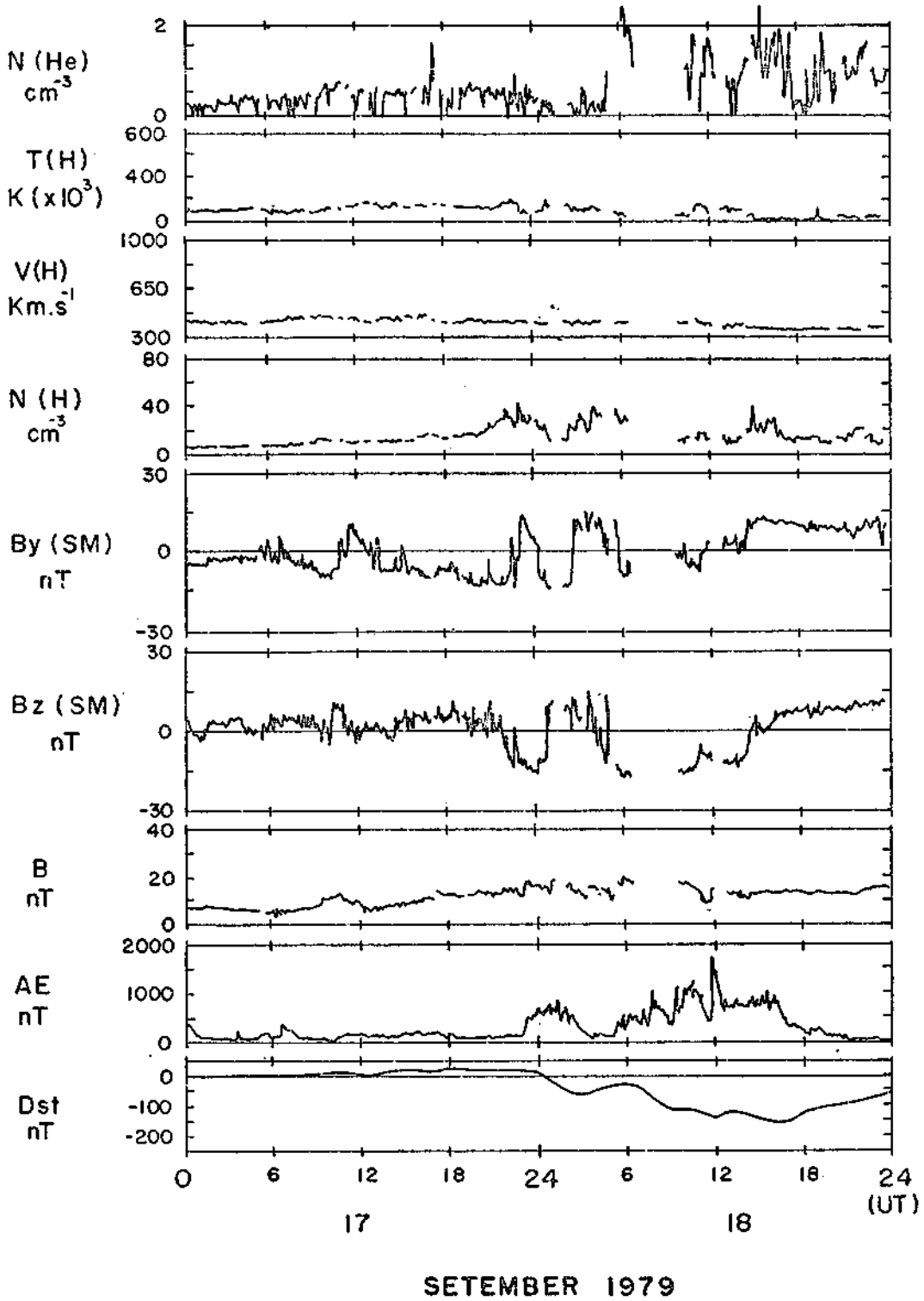
N (He)
cm-3
2
0
T(H)
K (x10^3)
600
400
0
V(H)
Km.s-1
1000
650
300
N (H)
cm-3
80
40
0
By (SM)
nT
30
0
-30
Bz (SM)
nT
30
0
-30
B
nT
40
20
0
AE
nT
2000
1000
0
Dst
nT
0
-100
-200
0
6
12
18
24
6
12
18
24
(UT)
17
18
SETEMBER 1979

Fig. 4